

Review

Microbial Efflux Pump Inhibitors: A Journey around Quinoline and Indole Derivatives

Giada Cernicchi, Tommaso Felicetti *  and Stefano Sabatini 

Department of Pharmaceutical Sciences, University of Perugia, Via del Liceo, 06123 Perugia, Italy; giada.cernicchi@outlook.it (G.C.); stefano.sabatini@unipg.it (S.S.)

* Correspondence: tommaso.felicetti@unipg.it; Tel.: +39-075-585-2185

Abstract: Antimicrobial resistance (AMR) is a complex threat to human health and, to date, it represents a hot topic in drug discovery. The use of non-antibiotic molecules to block resistance mechanisms is a powerful alternative to the identification of new antibiotics. Bacterial efflux pumps exert the early step of AMR development, allowing the bacteria to grow in presence of sub-inhibitory drug concentration and develop more specific resistance mechanisms. Thus, efflux pump inhibitors (EPIs) offer a great opportunity to fight AMR, potentially restoring antibiotic activity. Based on our experience in designing and synthesizing novel EPIs, herein, we retrieved information around quinoline and indole derivatives reported in literature on this topic. Thus, our aim was to collect all data around these promising classes of EPIs in order to delineate a comprehensive structure–activity relationship (SAR) around each core for different microbes. With this review article, we aim to help future research in the field in the discovery of new microbial EPIs with improved activity and a better safety profile.

Keywords: efflux pump inhibitors; antibiotic resistance breakers; microbial efflux pumps; antimicrobial resistance; antibiotic resistance



Citation: Cernicchi, G.; Felicetti, T.; Sabatini, S. Microbial Efflux Pump Inhibitors: A Journey around Quinoline and Indole Derivatives. *Molecules* **2021**, *26*, 6996. <https://doi.org/10.3390/molecules26226996>

Academic Editor: Patrick Loll

Received: 11 October 2021

Accepted: 17 November 2021

Published: 19 November 2021

Publisher's Note: MDPI stays neutral with regard to jurisdictional claims in published maps and institutional affiliations.



Copyright: © 2021 by the authors. Licensee MDPI, Basel, Switzerland. This article is an open access article distributed under the terms and conditions of the Creative Commons Attribution (CC BY) license (<https://creativecommons.org/licenses/by/4.0/>).

1. Introduction

The extensive use of antibiotics to treat microbial infections in humans and animals is paving the way to the development of resistant microorganisms. To date, antimicrobial resistance (AMR) represents a complex global public health issue with high costs for the healthcare sector, and the wider societal impact still largely unknown [1]. As a result of multidrug-resistant microbial infections, about 700,000 people worldwide die each year [2], 33,000 of which die in Europe, burdening the European Union with costs of EUR 1.5 billion annually [3]. Similarly, in the United States, more than 2 million people are infected with antibiotic-resistant microorganisms each year, with 35,000 deaths and an yearly cost to the health system estimated at USD 21 to USD 34 billion, coupled with more than 8 million additional days in hospitalizations [1].

To face AMR, besides discovering novel antibacterial agents, an alternative/parallel strategy relies on the approach of targeting microbial mechanisms underlying resistance. The idea of freezing resistance would allow antibiotics, which generated the resistance, to work again, thereby renewing our armamentarium to fight microbial infections. Over the years, molecules targeting factors involved in AMR have been named in different ways: adjuvant molecules, helper compounds or antimicrobial resistance breakers (ARBs) [4–7]. All of them share the lack of any antimicrobial activity of their own and the ability to synergize by different mechanisms with known antimicrobials, thus restoring the lost activity against resistant strains. Since microorganisms evolve resistance only for compounds exerting bactericidal or bacteriostatic effects, the lack of the antimicrobial activity in ARBs appears to be a strength for their potential use [8]. In addition, the combination of an ARB with an antibiotic could likely reduce the doses of the latter, thereby mitigating its side effects. Consequently, the use of ARB appears advantageous, even considering the great number

of microbial proteins and factors not suitable for developing direct antibacterials, which could be exploited as promising targets [4]. In this regard, ARBs might also be considered as anti-virulence compounds when the mechanisms involved in AMR are associated with increased microbial virulence, thus suggesting their use as a mono-therapy [9]. The research for anti-virulence compounds exerting a poor selective pressure on microorganisms and potentially respecting gut microbiota is in its infancy, more so than the strategy to combine an ARB with an antibiotic, but this approach deserves much more attention [10].

However, the use of an ARB to fight AMR is challenging, owing to various potential issues, including the identification of correct biological assays demonstrating the effective ARB activity. Indeed, it is essential that the synergism between the ARB and the antibiotic relies on the expected mechanism of the ARB. Moreover, the candidate ARB molecule should overcome all the “journey” of a drug development and next potential drug–drug interactions or side effects when co-administrated with different antibiotics. However, the feasibility of this strategy can be sought in the success of the β -lactamase inhibitors [11], progenitor of the whole ARB class and currently deemed essential in the antibiotic therapy based on β -lactam antibiotics.

Considering their peculiar role in AMR development, efflux pumps (EPs) represent a valuable target for developing ARB agents. EPs are typical trans-membrane proteins present both in prokaryotic and eukaryotic cells. They require an energy source (i.e., proton motive force) to extrude noxious compounds, such as substances synthesized by host organisms and a large array of antimicrobial agents [12]. Based on the amino acid sequence similarities, predicted secondary protein structures and phylogenetic relationship, microbial EPs are divided into six different families: ATP-binding cassette (ABC) superfamily, major facilitator superfamily (MFS), multidrug and toxic compound extrusion (MATE) superfamily, small multidrug resistance (SMR) superfamily, proteobacterial antimicrobial compound efflux (PACE) family, resistance–nodulation–cell Division (RND) superfamily [13]. In contrast, when classified according to the energy source used to extrude substrates, EPs fall in two classes; the former utilizes the hydrolysis of ATP (ABC superfamily) while the second class is an electrochemical gradient of sodium ions or protons (all the other families) [14].

EP inhibitors (EPIs) are to be considered a class of ARBs that may hold a pivotal role in fighting AMR. Since they are expressed in all microorganisms at a basal level, EPs are involved in several pathways functional to the microbial life [15]. However, during antibiotic treatment, the basal presence of EPs contributes to slightly decreased antimicrobial concentrations inside the microbial cells to sub-inhibitory levels, in turn producing an increase in the mutational transformations in microorganisms and promoting the development of target-based resistance [16–20]. Moreover, through the use of EPIs, the role of EPs in biofilm formation has been indirectly shown, by observing that pathogens overexpressing EP genes display a thicker biofilm than corresponding wild-type and EP genes knock-out strains. Although the mechanisms by which EPs contribute to the formation of biofilm are still unclear, the possibility that an EPI could inhibit biofilm is very intriguing [21–23].

Therefore, an EPI potentially appears effective: (i) in reducing insurgence of resistance in wild-type strains, (ii) in overcoming efflux-mediated mechanisms in resistant strains and (iii) in hindering biofilm production.

However, the downside underlying the development of an ARB, such as an EPI, relies on the poor availability of quick and smart biological screenings able to identify active molecules early. In addition, in literature, molecules have often been described as EPIs when they are not owing to the poor knowledge of the efflux mechanisms and the lack of biophysical experiments validating a true EP inhibition. Thus, the presence of “fake” EPIs in literature is (i) facilitated by the poor experience in this field due to its novelty and (ii) encouraged by the exhausting research of molecules fighting AMR and by the fascinating approach underlying the identification of ARBs.

Among the hundreds of papers reported in literature on this topic, we noticed the presence of two scaffolds which were most employed to design and synthesize new synthetic EPIs. Accordingly, based on our experience in the search for EPIs, we collected information about the derivatives reported in literature as microbial EPIs and characterized by these two scaffolds (quinoline and indole) in order to highlight the potential of these classes for the development of potent EPIs. For a comprehensive description of all microbial EPIs present in literature, we suggest some recent review articles [10,24,25]. Indeed, herein, we focused the attention on the delineation of a clear structure–activity relationship (SAR) around quinoline and indole derivatives as microbial EPIs. Since an EPI should not possess any antibacterial activity on its own, all described derivatives are to be considered as not possessing this activity, unless indicated. Great attention has been given to the experiments proving EPI activity and to the evaluation of the toxic profile. In order to compare EPI activities, when possible, the synergistic activity of EPIs with antibiotics has been furnished as minimal potentiating concentration (MPC) able to reduce x -fold the antibiotic minimal inhibitory concentration (MIC) (MPC_x). Below, EPI derivatives have been classified on the basis of the microorganisms where they are tested. In Table 1, all the microorganisms used to assess EPI activity for the cited compounds are reported. In addition, in Table S1, chemical names and structures of all described EPIs are reported.

Table 1. Description of the cited strains.

Strains	Description	Ref.
<i>B. subtilis</i>		
$\Delta\Delta$	genes that encode the multidrug transporters Bmr and Blt are genetically inactivated	[26]
$\Delta\Delta$ NA	expresses a functional NorA transporter from the plasmid expression vector pBEV	[27]
<i>S. aureus</i>		
SA-1199	wild-type	[27]
SA-1199B	overexpresses the chromosomal <i>norA</i> gene which harbors a mutation in <i>grlA</i>	[28]
8325-4	wild-type	[29]
K1758	Δ <i>norA</i>	[30]
K2361	SA-K1758 with pK364: <i>norA</i>	[31]
ATCC 25923	wild-type	
SA-K2378	having a plasmid that results in overexpression of <i>norA</i> from <i>S. aureus</i> SA1199	[32]
SA-K1902	Δ <i>norA</i>	[32]
<i>E. aerogenes</i>		
ATCC 13048	wild-type	
ATCC 13048 p9	overexpressing the EP activator <i>marA</i> gene	[33]
EA27	overexpressing EP, clinically isolated	[34]
EA3	overexpressing EP, clinically isolated	[34]
EA5	overexpressing EP, clinically isolated	[34]
CM-64	resistant to CAF due to EP overexpressing,	[35]
EA117	low porin levels and also substitutions in the QRDR domain of GrlA	[36]
EA289	overexpressing AcrAB–TolC pump	[36]
<i>E. coli</i>		
AG100	wild-type	
AG100A	AcrAB pump-deficient	[37]
AG100 _{tet}	overexpressing efflux pump	[38]
ATCC 25922	wild-type	
YD02	multidrug-resistant after induction from ATCC 25922	[39]
<i>P. aeruginosa</i>		
ATCC 27853	wild-type	

Table 1. Cont.

Strains	Description	Ref.
KP55	<i>K. pneumoniae</i> porin deficient phenotype	[40]
ATCC 700084	<i>M. smegmatis mc²155</i> wild-type	[41]
104	<i>M. avium</i> wild-type	[42]
104 _{CLA3}	resistant to CLA due to overexpression of efflux pumps	[43]
104 _{CLA4}	resistant to CLA due to overexpressing efflux pumps and harboring the mutation A-2059G in 23S rRNA	[43]

2. *Staphylococcus aureus* Efflux Pump Inhibitors

S. aureus is a Gram-positive bacterium belonging to the family of Staphylococcaceae. Grouped among the ESKAPE pathogens [44], *S. aureus* and especially its methicillin resistant strain (MRSA) are a great problem for the human health. It possesses several EPs belonging to different families, and some of them are able to extrude a wide array of compounds including many antibacterials commonly used in therapy and antiseptics. Indeed, the impact of EPs in the development of resistance in *S. aureus* is widely recognized, especially when considering their large overexpression in MRSA strains [45,46]. Among all the *S. aureus* EPs, NorA and MepA are the mostly studied and mainly involved in fluoroquinolone resistance. NorA consists of 388 amino acid residues and, as an MFS member, it is organized in 12 TM α -helices [47,48]. To date, no crystal structures are available, and little is known about the mechanism of efflux apart from how it functions by using the proton motive force. Over the years, many NorA EPIs have been discovered by three different approaches: (i) by screening libraries of natural or synthetic molecules; (ii) by repurposing molecules with known biological activity and (iii) by designing and synthesizing new compounds. The lack of an NorA crystal structure has strongly hampered the identification of potent NorA EPIs with no examples of structure-based drug design reported for EPI identification, which, therefore, relies on ligand-based drug design approaches or classical medicinal chemistry strategies. However, some efforts have also been directed towards the development of homology models coupled with computational studies to (i) perform virtual screening of potential NorA EPIs, (ii) propose the binding mode of some molecules inside the NorA EP, and (iii) understand how NorA could extrude its substrates [49–51].

2.1. Indole Derivatives

In 1999, the pioneering group of Neyfakh [52] performed a screening on 9,600 structurally diverse compounds with molecular weights ranging from 200 to 700 against a modified strain ($\Delta\Delta$ NA) of *B. subtilis* expressing the *norA* gene from a plasmid [53].

$\Delta\Delta$ NA strain derives from the previously built *B. subtilis* $\Delta\Delta$ strain, where genes encoding the two main EPs Bmr and Blt have been inactivated [54]. By this modification, $\Delta\Delta$ NA strain exhibited a 20-fold increase in resistance to ethidium bromide (EtBr—Figure 1) with respect to its parent $\Delta\Delta$ strain.

Each compound was tested at the concentration of 20 $\mu\text{g}/\text{mL}$ in combination with EtBr at 10 $\mu\text{g}/\text{mL}$, a concentration four-fold lower than its MIC [52]. Since the only known resistance mechanism for EtBr is its pump-mediated extrusion, the authors quickly identified which derivatives exhibited NorA EPI activity. In addition, specific NorA inhibition was assured because genes encoding for other EPs were silenced. Out of 9600 derivatives, 399 showed a four-fold EtBr MIC reduction while not having any bactericidal effect at the used concentrations. When checkerboard assays were performed with ciprofloxacin (CPX—Figure 1), 28 compounds retained activity up to 5 $\mu\text{g}/\text{mL}$, such as the reference compound reserpine (RES—Figure 1), while 11 of the 399 derivatives showed a higher EPI activity than RES, as they were still effective at 2.5 $\mu\text{g}/\text{mL}$.

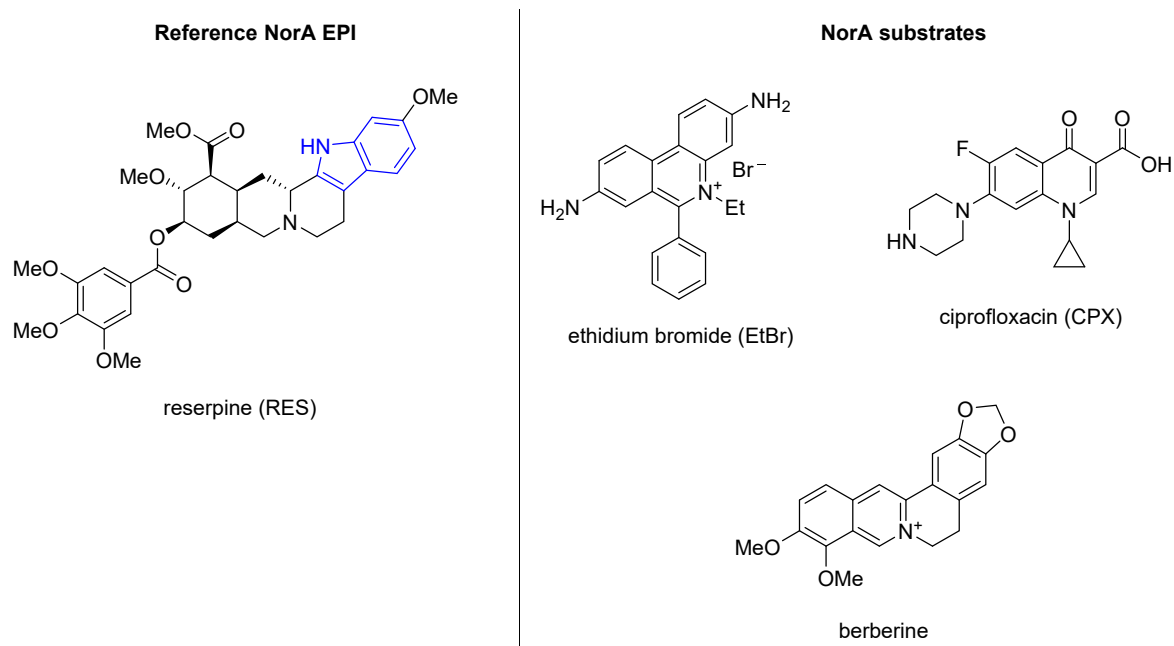


Figure 1. Reference NorA EPI reserpine (RES) and NorA substrates ethidium bromide (EtBr), ciprofloxacin (CPX) and berberine. Blue color is used to highlight the indole portion present in reserpine.

Interestingly, among the 399 active compounds, 30 possessed an indole ring such as RES, and 11 derivatives were endowed with a biphenyl urea moiety. After checkerboard assays, in combination with CPX against SA-1199B, indole derivative **1** (Figure 2) resulted in one of the best compounds endowed with an MPC₄ of 1.5 µg/mL. In addition, **1** was also able to prevent a fluorescence decrease in EtBr efflux assays on the ΔΔNA strain, similarly to RES. Unfortunately, the authors did not carry out a cytotoxicity evaluation on human cells, thereby foreclosing a potential use in in vivo models.

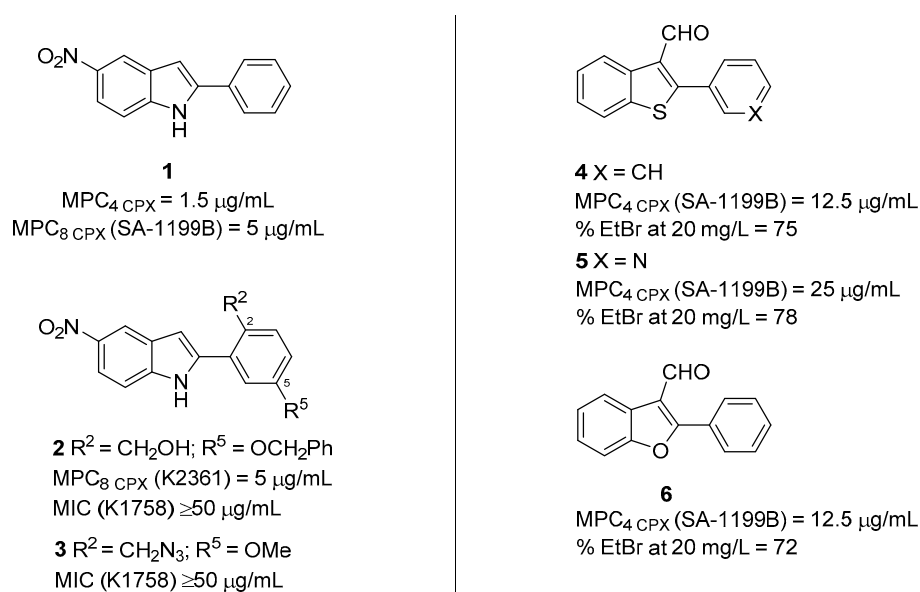


Figure 2. From indoles to benzothiophene and benzofuran EPIs.

In 2005, Samorson et al. [55] explored the C-2' and C-5' positions of the phenyl ring on the C-2 position of the indole nucleus of derivative **1**, synthesizing a set of 10 derivatives. Compounds devoid of any antibacterial effect on their own (MIC ≥ 50 µg/mL) against

three different *S. aureus* strains (K1758, 8325-4 and K2361—Table 1) were evaluated for their synergistic activity with berberine (a known NorA EP substrate—Figure 1). Compounds 2 and 3 (Figure 2), characterized by the presence on the C-2 phenyl ring of a primary alcohol or an azidomethyl group at the C-2' position and of a benzyloxy or methoxy substituents at C-5' position, respectively, emerged as the best derivatives able to potentiate berberine more than 15-fold (from >500 to 30 µg/mL) at a concentration of 0.8 and 1.5 µg/mL, respectively, against K2361 (Table 1). While a primary alcohol or an azidomethyl group were well tolerated at C-2' coupled with a benzyloxy or methoxy substituents at C-5', an acidic function at C-2' resulted in the lack of berberine potentiation. On the other hand, regardless of substituent at C-5' phenyl ring, a primary amine at C-2' yielded derivatives with synergistic activity against *S. aureus* strains wild-type and *norA* deleted while lacking EPI activity against K2361 (Table 1). The best compound 2 was further evaluated, in comparison with 1, for its ability to promote berberine accumulation and to synergize with CPX in the used *S. aureus* strains. Like 1, derivative 2 showed a CPX MPC₈ of 5 µg/mL and it was able, at 10 µg/mL, to promote berberine accumulation on K2361 strain (overexpressing *norA*—Table 1). However, a careful analysis of berberine accumulation curves showed that activity of compounds 1 and 2 could not be only due to NorA inhibition. Indeed, berberine accumulation in the three used strains only occurred in Δ *norA* strain K1758 (Table 1) producing values of relative fluorescence unit (RFU) of about 200 after 20 min, while no fluorescence was recorded in the wild-type *S. aureus* 8325-4 and *norA*++ K2361 strains (Table 1), indicating that berberine was completely extruded. When compounds 1 and 2 were tested at 10 µg/mL as the final concentration, RFUs drastically increased at values above 500 on all the used strains. Therefore, since the addition of compounds 1 and 2 caused such a high increase in the fluorescence in all strains (also those wild-type and Δ *norA*), the effect of berberine accumulation may be nonspecific for at least three different reasons. Indeed, compounds 1 and 2 could: (i) increase membrane permeability of *S. aureus* cells, thereby nonspecifically synergizing with berberine; (ii) also inhibit EPs other than NorA involved in berberine extrusion; (iii) emit fluorescence at the same wavelength as berberine. Unfortunately, no data about cytotoxicity against human cells was available.

One year later, on the back of the good results obtained around the nitro-indole moiety as essential scaffold for NorA EPI activity, Fournier et al. [56] undertook an extensive synthetic effort to develop arylbenzo[b]thiophene and diarylthiophene derivatives with the aim to evaluate the importance of the indolic nitrogen atom for NorA inhibition. No compounds showed any antibacterial effect at concentrations lower than 100 µg/mL against *S. aureus* ATCC 25923 (Table 1); however, no MIC values were determined against SA-1199B (Table 1), the *S. aureus* strain used for synergistic assays, thus making it impossible to ascertain, though synergism was influenced by a direct antibacterial activity. A key requirement to possess synergistic activity in the arylbenzothiophene class was the presence of an aldehyde group at C-3 position coupled with substitutions on the C-2 phenyl ring in para position rather than meta or ortho positions. However, compounds with the aldehyde group at C-3 and an unsubstituted C-2 phenyl ring (4—Figure 2) or a C-2 pyridin-3-yl portion (5—Figure 2) showed promising MPC₄ values (\leq 25 µg/mL). On the other hand, benzothiophene derivatives bearing -CN, a -OCH₃, or a -OCH₂CF₃ groups at C-3 or even aryl moiety shifted from C-2 to C-3 exhibited MPC₄ values \geq 50 µg/mL. Interestingly, when the main nucleus was shrunk by benzene removal to give thiophene derivatives, the synergistic effect was completely lost, regardless of substituents. On the contrary, sulphur replacement of the benzothiophene with an oxygen atom yielded the benzofuran derivative (6—Figure 2) that retained the same activity as its close structural analogue 4. For the best compounds 4-6, NorA inhibition at 20 µg/mL was confirmed by EtBr efflux assays in comparison with RES. Finally, the cytotoxic profile was assessed for a large panel of derivatives against three different cell lines: keratin-forming tumor HeLa (KB), breast cancer (MCF7) and breast carcinoma (MCF7R). Unfortunately, derivatives 4 and 6, at lower concentrations (10 µM) than those needed for NorA inhibition, showed a significant

inhibition of the human cell growth. The only exception was derivative **5**, which exhibited a weak inhibition of KB cell growth and no significant effect against MCF7 and MCF7R; however, the tested concentration for cytotoxic assessment was about 10-fold lower than its MPC₄. Thus, although the authors reported arylbenzo[*b*]thiophene derivatives as NorA inhibitors for the first time, much needs to be done to improve this chemical class to obtain more potent and safer compounds. Moreover, the authors should reconsider the initial assumption to remove the –NO₂ group present in indole **1** in an attempt to increase NorA EPI activity. Indeed, a direct comparison of the EPI activity of **1** with the best benzothiophene derivative **4** highlights that indole moiety is preferred over the benzothiophene nucleus, even though the presence of the –NO₂ group of **1** as well as the aldehyde of **4** could influence EPI activity, thereby hampering the comparison between the two nuclei.

In 2008, as a continuation of the previous study [55], the group of Lewis [57] reported the synthesis and biological evaluation of 20 new 2-aryl-1*H*-indole derivatives with the aim to investigate the role of the –NO₂ group in modulating the indole-mediated NorA inhibition. Thus, after the synthesis and evaluation of eight indole derivatives with different substituents at the C-5 position, the authors identified the –NO₂ group as essential to possessing synergistic activity, in combination with berberine against the *S. aureus* wild-type (8325-4) and *norA* overexpressing (SA-K2378) strains (Table 1), with only the CN group that is potentially able to replace the NO₂ group. Accordingly, the authors synthesized six new nitro-indole derivatives and their corresponding des-nitro compounds bearing different substituents on the C-2 aryl moiety. Synergistic activity, in combination with berberine, was evaluated as the MPC_{13.3} for each compound. As expected, all des-nitro indole derivatives showed poor synergistic activities, while nitro-indole analogues highlighted moderate to good effects. In particular, although less active than starting hit **1**, derivatives **7** and **8** (Figure 3) displayed an MPC_{13.3} of 1.0 μM (0.3 μg/mL) and 2.0 μM (0.5 μg/mL), respectively, against both *S. aureus* 8325-4 and SA-K2378 (Table 1). This comparable activity against the two used strains clearly highlights that both compounds have a nonspecific synergizing effect, as they reduce berberine MIC in the same manner against the wild-type and the *norA* overexpressing strains. In addition, although all compounds exhibited MIC values much higher than concentrations needed to reach the synergistic effect with berberine, the NorA inhibition was not proved by EtBr efflux assays for any of the compounds. No data about synergistic activity with CPX or other NorA antibacterial substrates was reported.

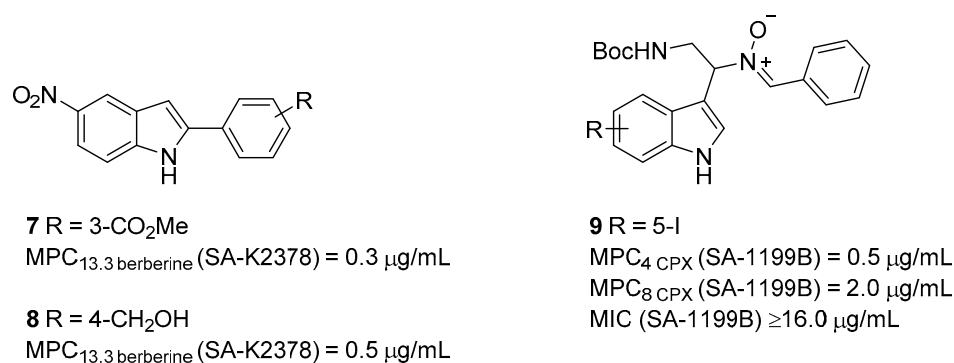


Figure 3. Indoles derivatives as NorA EPIs.

In 2014, Hequet et al. [58] further explored the role of the indole derivatives as NorA EPIs, focusing attention on the C-3 position. From a previous work aimed at discovering new indoles as antibacterial agents, the authors observed that the presence of an aldonitrone moiety at the C-3 position removed the antibacterial activity against different bacteria [59]. With the aim to improve solubility, they enlarged the indole series, further synthesizing 12 new indole analogues that were tested as NorA EPIs by evaluating their

ability to inhibit, alone or in combination with CPX, the bacterial cells' growth against SA-1199B strain (Table 1). By analyzing the synergistic activity of compounds at concentrations below their MIC values, it is possible to state that the presence of a halogen atom at C-5 position of the indole core is essential to displaying NorA EPI activity (best compound **9** MPC₄ = 0.5 µg/mL, MPC₈ = 2.0 µg/mL, MIC > 16.0 µg/mL—Figure 3). Indeed, derivatives, where the halogen atom was removed, showed a poor synergistic activity with CPX against SA-1199B (Table 1). This behavior is consistent with the importance of an electron-withdrawing group at the indole C-5 position, as also shown by the –NO₂ group of derivative **1**. Furthermore, the indole derivative with halogen at C-6 retained significant synergistic activity (MPC₄ = 4.0 µg/mL), strengthening the key role of the halogen on the indole core. On the other hand, aldonitrone moiety at C-3 was not essential to imparting NorA inhibition activity; indeed, when it was replaced with hydroxylamine or amide functions, synergistic activity with CPX against SA-1199B was not affected. However, in order to investigate whether the best derivatives specifically inhibited NorA function, the authors performed checkerboard assays for these compounds against SA-K2378 (*norA*+) (Table 1) and EtBr accumulation assays against SA-1199B (Table 1). All of them exhibited good synergistic activities with CPX and EtBr accumulation, thus confirming their mechanism of action as NorA EPIs. Cytotoxicity evaluation at 10 µM against three different human cell lines (human lung fibroblast—MCR5, human mouth carcinoma—KB and human colon tumor—HCT116) disclosed that the best compounds (including **9**) showed cytotoxic activity against human cells.

Two years later, based on a previous work aimed at obtaining the 6-bromobenzo[*b*]thiophene-3-carbonitrile intermediate for Raloxifen synthesis [60], Liger et al. attempted to optimize the previously identified arylbenzo[*b*]thiophene derivatives (i.e., **4**) [61]. Although benzothiophene derivatives bearing a –CN group at C-3 did not show any NorA EPI activity in their previous work [56], the authors synthesized and tested a wide set of cyanobenzothiophene derivatives. However, the C-3 position was widely decorated with different electron-withdrawing groups in combination with an array of substituents, mainly at the C-6 position but also at C-4 and C-5. Once they excluded any antibacterial effect for all derivatives against ATCC 25923 and SA-1199B strains (Table 1), the authors assessed the synergistic effect of the compounds with CPX against SA-1199B. Although it was impossible to delineate a clear SAR around this class due to a lack of correlation between the activities of the combined substituents, some compounds showed promising synergistic activities at low concentrations. In particular, compounds **10** and **11** (Figure 4) exhibited an MPC₈ of 1 µg/mL and an MPC₁₆ of 2 µg/mL while showing an MIC > 128 µg/mL on tested strains. For both compounds, NorA inhibition was confirmed by EtBr accumulation assays at 20 µg/mL on SA-1199B by using RES as positive control. However, no synergistic assays against *S. aureus* strains wild-type or lacking NorA pump were performed, thereby not fully demonstrating the absence of a possible secondary synergistic mechanism, such as the increase in membrane permeability. Moreover, no human cell toxicity was assessed.

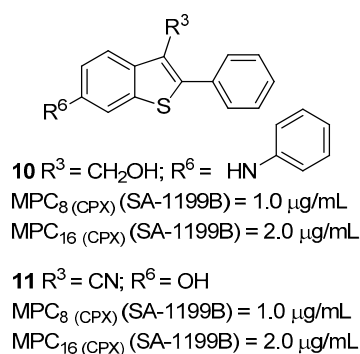


Figure 4. Benzothiophene derivatives as NorA EPIs.

In 2016, based on the literature data reported over the years around the indole core, Lepri et al. planned a rational design aimed at obtaining potent indole-based NorA EPIs [62]. The authors performed a wide effort to enrich SAR information around the indole core using a four-step design protocol, especially focusing attention on the *N*-1, C-3 and C-5 positions. The first substantial modification entailed the shift of the aryl from C-2 position, as the most potent indole EPIs **1-3** (Figure 2), to *N*-1 position of the indole core after demonstrating a similar spatial occupancy by superimposing the new *N*-benzyl indole with the 2-phenyl indole using FLAP software [63]. Thus, a set of benzyl-indole derivatives with an ethylic ester function at C-3 was synthesized with different substituents at the C-5 position in order to verify the role of the $-\text{NO}_2$ group (present in **1**). All derivatives showed poor **EtBr** efflux inhibition at 50 μM against SA-1199B, with the exception of **12** bearing at C-5 a diethylamino ether chain (Figure 5). Interestingly, the indole derivative **13**, the direct analogue of **1** within this series of compounds and with the $-\text{NO}_2$ group at C-5, was found to be inactive, thereby highlighting that the shift of the aryl moiety from C-2 to *N*-1 was detrimental (Figure 5). Although derivative **12** was the first indole NorA EPI derivative with an electron-donating group at C-5, the effect did not appear to be due to the electron-donating property of the C-5 substituent since other derivatives did not show any NorA EPI activity. On the contrary, the NorA EPI activity of derivative **12** would appear to be related to the presence of the protonable alkylamino chain, which was previously identified in the quinoline scaffold (see below) and is essential to imparting NorA inhibition [64]. Thus, the authors focused their attention on the substituent at C-5, introducing several different *O*-alkylamino chains. Overall, all 22 derivatives retained an excellent **EtBr** efflux inhibition, proving the key role of the protonable alkylamino chains in obtaining NorA inhibition.

Further modifications showed that the removal of the benzyl moiety from *N*-1 position led to a completely inactive derivative, thereby highlighting the importance of a lipophilic portion in this position. In addition, the removal or the hydrolysis of the ester at C-3 led to an increase in the antibacterial activity or the lack of **EtBr** efflux inhibition, respectively. Substitutions on the benzyl moiety gave few differences in terms of **EtBr** efflux inhibition regardless of the position of the substituent and its chemical property. Before selecting the best derivatives to evaluate their synergistic activity with **CPX** against SA-1199B (Table 1), the authors performed ADME studies on the best compounds overall, observing a moderate to good human metabolic stability after 30 minutes. However, the authors selected only some compounds to be evaluated for their synergistic activity, with **CPX** against SA-1199B and the wild-type SA-1199 (Table 1). The three derivatives (**14** included as representative) (Figure 5) showed an MPC_4 of 3.13 $\mu\text{g}/\text{mL}$ and an MPC_8 of 12.5 $\mu\text{g}/\text{mL}$ against SA-1199B while not showing any significant synergistic effect against the wild-type SA-1199.

In conclusion, the authors performed a wide effort to enrich SAR around the indole core and identified new indole derivatives with good NorA inhibition, even without the $-\text{NO}_2$ group at C-5. The best derivatives showed synergistic activity comparable to the starting hit **1** but, unfortunately, the authors did not deepen the studies around these compounds to confirm if their synergistic activity was due to the NorA inhibition by checkerboard assays against *norA* knock-out and *norA* overexpressing *S. aureus* strains. Nevertheless, the wide SAR work has strengthened the information in a view to obtain more potent indole-based NorA EPIs.

One year later, starting from the good **EtBr** efflux inhibition activity of the side product **15** (Figure 5) obtained during the synthesis of some derivatives in the previous work [62], the same authors planned a rational design aimed at performing a scaffold-hopping approach to obtain unsymmetrical derivatives of **15** [65]. Thus, through a virtual screening on the SPECS database using FLAP, authors identified two fragments to replace the symmetric portion of **15** in order to synthesize derivatives **16** and **17** (Figure 5), which unfortunately showed poor **EtBr** efflux inhibition. Thus, after a chemical optimization, derivatives **18** and **19** (Figure 5) showed an excellent **EtBr** efflux inhibition (low $\text{IC}_{50\text{s}}$) coupled with high MIC values. Synergistic activity with **CPX** against SA-1199B was reported with FIC values,

thus making difficult to obtain the exact MPC value for each compound. In addition, no synergistic evaluation was performed against specific *norA* knock-out and overexpressing strains as also in the previous work [62].

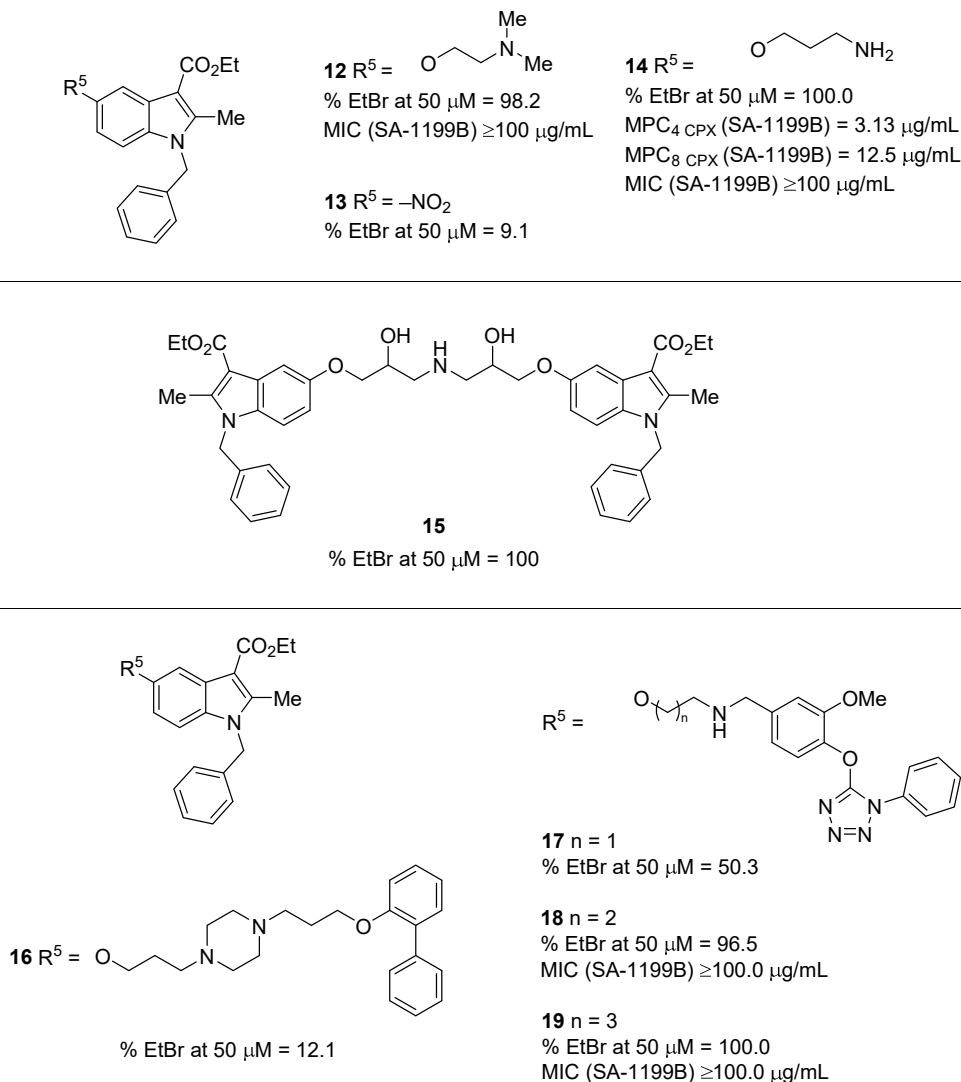


Figure 5. *N*-1 substituted indole derivatives as NorA EPIs.

Taking into account all the indole analogues reported over the years as NorA EPIs, we tried to build a comprehensive SAR, as depicted in Figure 6. Since many groups focused their efforts on the identification of indole derivatives as NorA EPIs, SAR information is often related to the series of each research group, making it difficult to rationalize clear guidelines to design potent NorA EPIs. However, it is interesting to note that the indole core can be also replaced by benzothiophene or benzofuran moieties if properly substituted. On the other hand, regarding the indole core, the presence of a NO₂ group at the C-5 position appears essential when a phenyl moiety is at C-2, while *O*-alkylamino chains at C-5 yielded potent derivatives when coupled with the aromatic portion shifted to the *N*-1 position. Of note, a carboxylic function was always poorly tolerated, affording derivatives lacking NorA EPI activity.

2.2. Quinoline Derivatives

Inspired from the 2-phenyl-4*H*-chromen-4-one, a common scaffold of the flavone and flavolignane EPIs [66], in 2011, Sabatini et al. started their work around the quinoline derivatives as potent NorA EPIs [67]. Initially, by replacing the endocyclic oxygen of

the chromene core with a nitrogen atom, the 2-phenylquinolone core was obtained and, subsequently, decorated with different polar chains based on the promising results of some MDR inhibitors [68]. During the synthesis of the *N*-alkylated quinolones, *O*-alkylated 2-phenylquinoline derivatives were also obtained, proving to be the best NorA EPIs of the series. Indeed, derivatives **20** and **21** (Figure 7), devoid of any antibacterial activity on their own, showed the best results in terms of both **EtBr** efflux inhibition and synergistic activity with **CPX** against SA-1199B (MPC₄ of 6.25 and 1.56 µg/mL, respectively). Therefore, an initial SAR around the quinoline core was delineated with alkylamino chains boosting the NorA EPI activity when present on the oxygen at the C-4 position (i.e., derivatives **20** and **21**), rather than at the *N*-1 position or on the oxygen at the C-4' position of the C-2 phenyl ring. In parallel, the best substituent for the C-4' position of the C-2 phenyl ring was a *-OPr* group, which was preferred over a free *-OH* or other alkyl ethers such as *-OMe* or *-OEt*. Noteworthy, derivatives **20** and **21** also showed good synergistic activity with **CPX** against SA-K2378 (Table 1) while no significant effect was observed against the *S. aureus* strains where NorA was poorly or not present (SA-1199 and SA-K1902—Table 1).

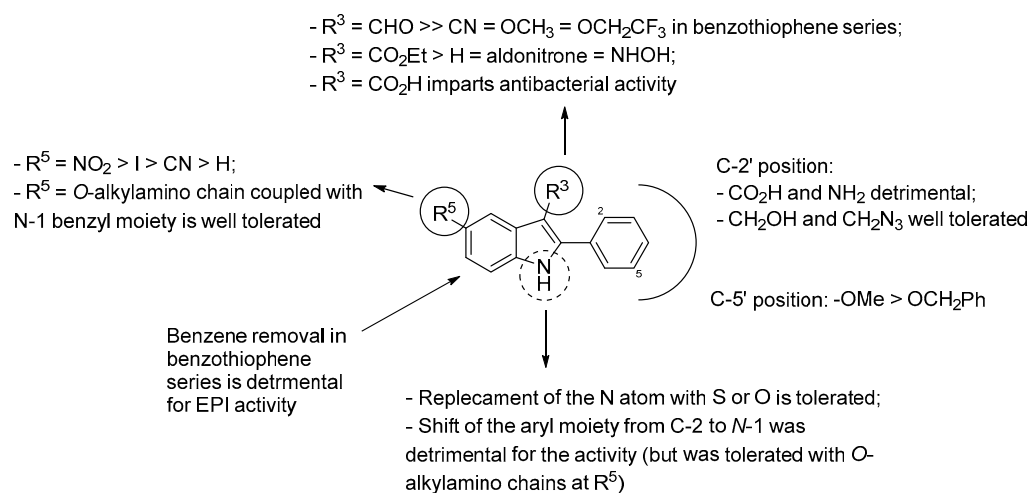


Figure 6. SAR of indole derivatives as NorA EPIs.

Further optimization focused on the oxygen at the C-4 position of the 2-phenylquinoline core led to the design and synthesis of a wide set of analogues with different *O*-alkylamino chains [64]. When tested for evaluating their **EtBr** efflux inhibition and synergism with **CPX** against SA-1199B (Table 1), most of the compounds showed excellent results. In particular, derivatives **22** and **23** (Figure 7) showed MIC values ≥ 100 µg/mL, an MPC₄ of 0.78 µg/mL and an **EtBr** efflux inhibition of about 90% at 50 µM. In addition, both compounds exhibited excellent synergistic activity with **CPX** against SA-K2378 (Table 1) and no effect against the other *S. aureus* strains with poor or no NorA expression (SA-1199 and SA-K1902, respectively—Table 1).

Once it was reported that *O*-alkylamino chains at C-4 position were needed to impart NorA EPI activity to quinoline derivatives, further efforts were directed towards the functionalization of the “naked” benzene ring of the quinoline core [69]. Based on the large presence of the *-OMe* group on different known NorA EPIs, the functionalization of the quinoline C-5, C-6, C-7 and C-8 positions with *-OMe* groups was planned, maintaining *p*-*OPr* group at C-2 phenyl ring and selecting the best *O*-alkylamino chains at C-4. Biological assays showed that the *-OMe* introduction on the quinoline core yielded more potent NorA EPIs than des-methoxy analogues. In particular, the introduction of one *-OMe* at C-6 or two *-OMe* groups at the C-6 and C-7 positions resulted the best combinations, with compounds **24** and **25** (Figure 8) that emerged as the best derivatives, showing an **EtBr** efflux inhibition $\geq 90\%$, high MIC values (100 and >100 µg/mL, respectively) and an MCP₈ of 0.78 µg/mL against SA-1199B (Table 1). In parallel, both compounds exhibited high synergism with **CPX** against SA-K2378 and no effect against SA-1199 and SA-K1902

(Table 1). Interestingly, compounds **24** and **25** also showed a non-toxic profile when tested on human liver epithelial (HepG2) cells, exhibiting CC_{50} values of 42.0 $\mu\text{g}/\text{mL}$ for **24** and 74.0 $\mu\text{g}/\text{mL}$ for **25**. As a confirmation, CC_{50} values $> 100 \mu\text{g}/\text{mL}$ were observed against the human monocytic cell line (THP-1). Accordingly, both compounds possessed a CC_{50}/MPC_8 ratio > 128 -fold. Interestingly, at 0.78 $\mu\text{g}/\text{mL}$, neither compounds modified the membrane proton motive force needed for NorA function, thus disclosing that NorA inhibition was not due to a nonspecific effect. In addition, both compounds also showed EPI activity towards MepA EP. Guided by the promising results obtained with the 6-OMe derivative **24**, further efforts were directed towards the investigation of the C-6 position of the quinoline core [70]. Considering the essential role of the alkylamino chain at the C-4 position of the quinoline, different analogues were designed with two *O*-alkyl-basic chains at C-4 and C-6 positions [70]. In addition, the intermediates C-6 *O*-benzyl and free OH analogues were used as counterparts to investigate the SAR. Although almost all the derivatives showed excellent inhibition of the **EtBr** efflux at 50 μM , only C-6 benzyloxy derivatives **26** and **27** (Figure 8) exhibited potent synergism with **CPX** against SA-1199B (Table 1). Indeed, both of them showed an MPC_4 of 0.78 $\mu\text{g}/\text{mL}$ coupled with poor or no synergistic effect against the wild-type strains ATCC 25923 and SA-1199 (Table 1). Evaluation of the cytotoxicity on HepG2 cells disclosed a significant toxicity, with CC_{50} values of 12.26 $\mu\text{g}/\text{mL}$ (for **26**) and 33.83 $\mu\text{g}/\text{mL}$ (for **27**). However, the combination of CC_{50} values with MPC_4 suggested a promising selectivity of action for both compounds.

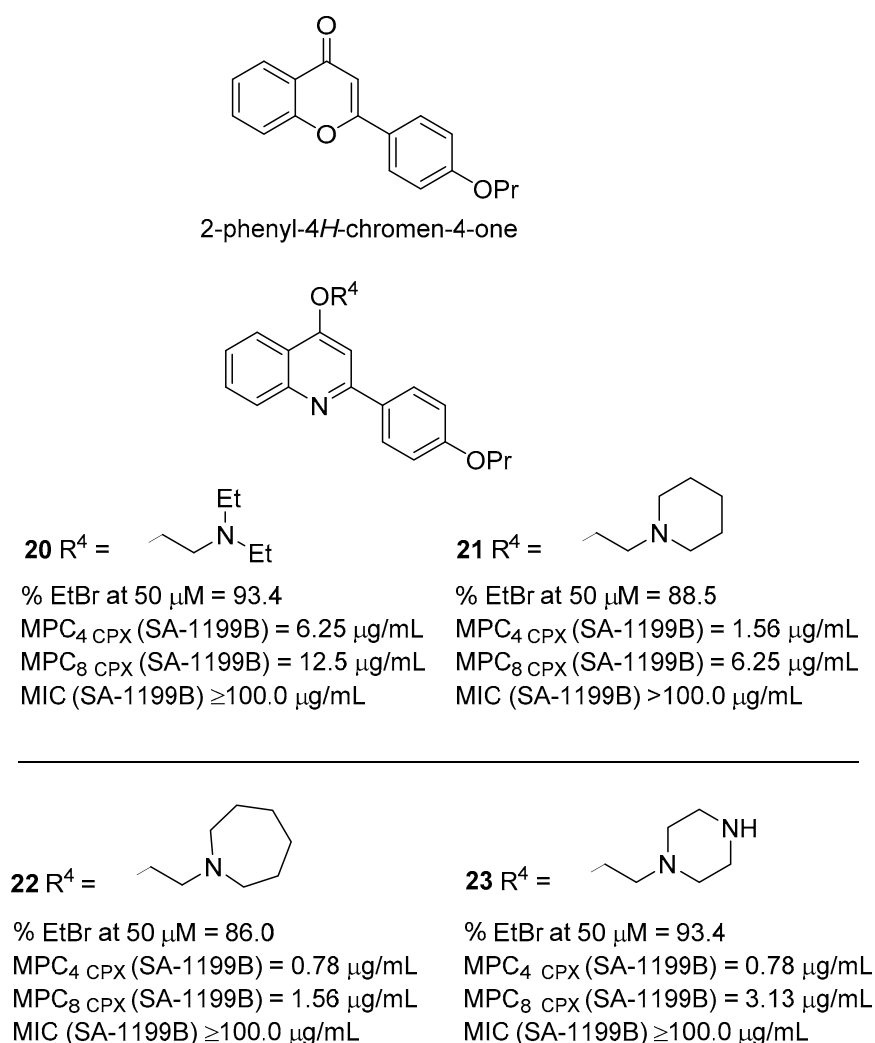


Figure 7. From flavone to quinoline nucleus.

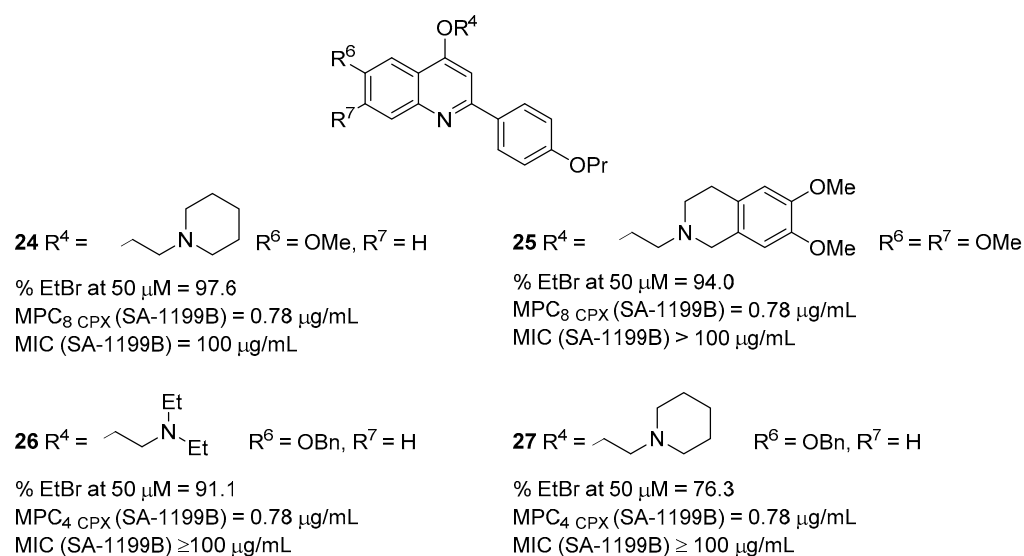


Figure 8. C6-modified O-alkylamino quinolines **24–27** as NorA EPIs.

Two years later, the same authors focused their efforts on the exploration of the C-2 position of the quinoline core by replacing the 4'-propoxyphenyl substituent with differently substituted pyridine or thiophene moieties [71]. Starting from **20** (Figure 7), 16 new analogues were designed and synthesized by combining eight new C-2 aryl quinoline scaffolds with two different chains at C-4 (O-ethyl-*N,N*-diethylamino and O-ethylpiperidine). In checkerboard assays with CPX, chlorothiophene derivative **28** (Figure 9) showed the best synergistic effect, with an MPC₄ of 0.39 μg/mL. By considering SAR information, the pyridine ring at the C-2 position was detrimental to NorA EPI activity, while thiophene moiety yielded some promising analogues, including the best compound **28**. NorA inhibition was confirmed on SA-1199B by: (i) EtBr efflux assays at 50 μM with **28** that showed an inhibition percentage ≥ 70% and (ii) membrane polarization assays with **28** depolarizing *S. aureus* membrane less than 20% when tested at 5 μg/mL. In addition, **28** exhibited a CC₅₀ value of 6.33 μg/mL on THP-1 cells, showing a promising CC₅₀/MPC₄ ratio of 16.

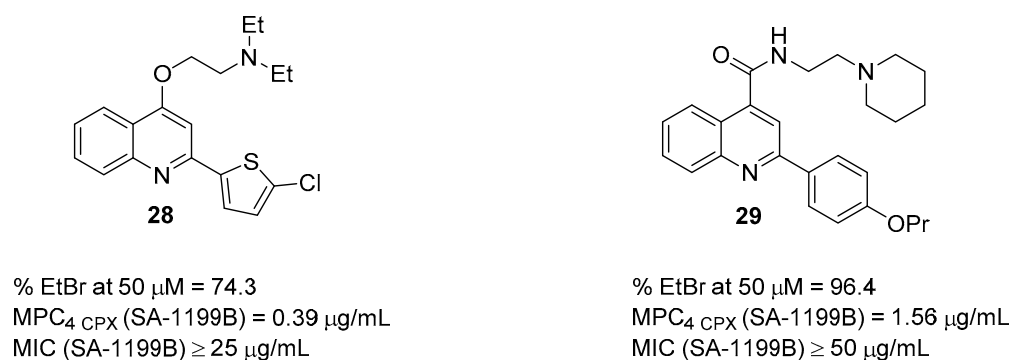


Figure 9. C-2 chlorothiophene-quinoline **28** and C-4 carboxy-quinoline **29** as NorA EPIs.

Recently, with the aim to enrich the array of NorA EPIs, the same research group performed a scaffold-hopping approach of the quinoline core followed by a pharmacophore-based virtual screening [72,73]. Therefore, the quinoline-4-yloxy core of **20** (Figure 7) was replaced by several scaffolds arising from the smart fragmentation of approved drugs to generate a virtual library that was screened on two previously reported pharmacophore models for NorA EPIs [74]. Virtual hits with nine different scaffolds (quinoline-4-carboxamides, phthalazin-1(2*H*)-ones, benzimidazoles, pyridine, 1,7-naphthyridine, 1,8-naphthyridine, isoquinoline and quinazoline) were synthesized and evaluated as NorA EPIs. Although 2-arylquinazoline were found to be the best derivatives, two quinoline-4-carboxamide

derivatives (compound **29** as representative) (Figure 9) showed promising synergism with CPX against SA-1199B with an MPC₄ of 1.56 µg/mL. In addition, EtBr efflux inhibition on SA-1199B was of 96%, while synergistic activity with CPX was not observed against *S. aureus* strains lacking *norA* gene, thus confirming NorA inhibition as the potential mechanism of action. Cytotoxicity was also measured on two different cell lines (THP-1 and A549), which, in the presence of **29** at 3.13 µg/mL, exhibited a vitality of 62 and 100%, respectively. In addition, experiments also showed that isoquinoline and pyridine derivatives completely lost NorA EPI activity, thus suggesting important SAR information.

Considering the high number of reported articles from the same research group about quinoline derivatives as NorA EPIs, SAR around this core was more robust than for indole derivatives. Indeed, the picture in Figure 10 fully describes the state of the art around the chemical information to obtain potent quinoline analogues as potent NorA EPIs. Briefly, since size core reduction to pyridine yielded inactive derivatives, we can consider the quinoline core as essential, even though quinazoline nucleus gave potent derivatives. The shift of the C-2 aryl moiety to the C-3 position afforded derivatives less potent as NorA EPIs, while improving NTM EPI activity (see below), similarly to what happens for the position of the alkylamino chain if moved from the oxygen at C-4 to the N-1 position.

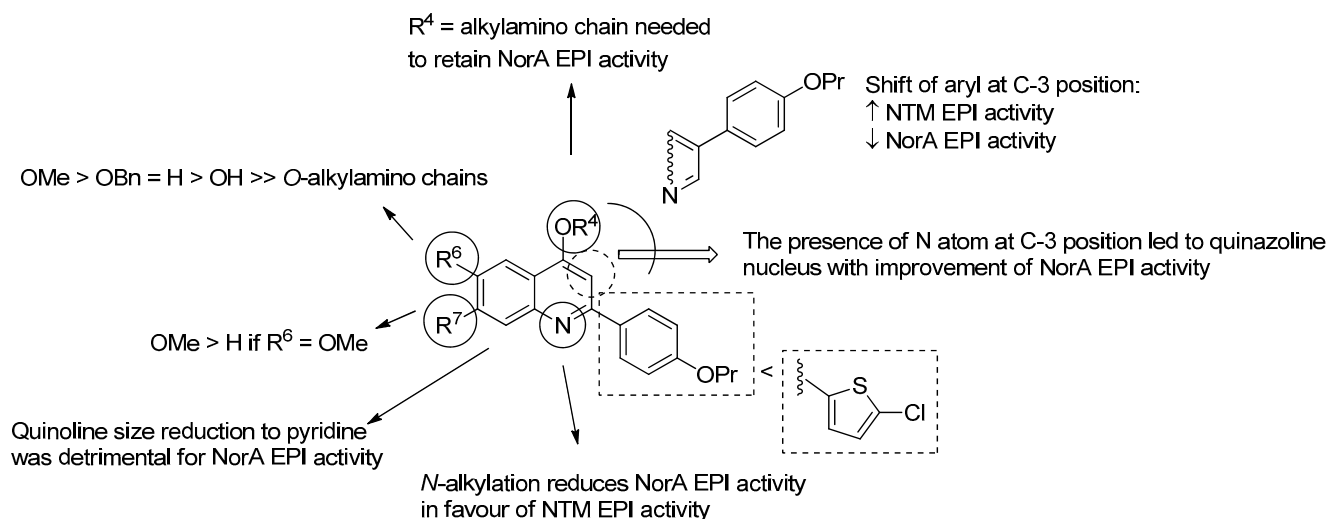


Figure 10. SAR of quinoline derivatives as NorA EPIs.

In addition, at the C-6 position, the introduction of a free OH group or a second O-alkylamino chain was detrimental to NorA EPI activity, while the presence of a OMe group improved the activity and was preferred over a benzyloxy or a hydrogen. Interestingly, a OMe group at the C-7 position was well tolerated when a second OMe group was at C-6; indeed, mono-methoxy C-7 derivatives were less active than des-methoxy analogues.

3. Gram-Negative Efflux Pump Inhibitors

In 2017, the WHO published a list of antibiotic-resistant priority pathogens, and among these, the majority belongs to the Gram-negative bacteria class. These bacteria can cause serious diseases, such as pneumonia, blood-stream infections, meningitis and peritonitis, particularly in immune-compromised individuals. The nosocomial infections caused by Gram-negative pathogens are the harder issue for healthcare professionals due to the capability of microorganisms to acquire resistance, making pharmacological treatments ineffective. Unlike Gram-positive bacteria, Gram-negative bacteria have an outer membrane (OM), which is the main reason for resistance to a wide range of antibiotics, such as β-lactams, quinolones, tetracyclines [75]. The OM contains porins and other proteins that allow the passage of small molecules as well as hydrophilic antibiotics, while hydrophobic drugs can pass through a diffusion pathway [76]. Therefore, the alteration of

hydrophobic properties coupled with structural mutations, including the overexpression of EPs, can contribute to the onset of resistance [77].

The most known EPs in Gram-negative bacteria are AcrB of *E. coli* and MexB of *P. aeruginosa*, belonging to RND family, whose crystal structures are available (PDB codes: 1IWG and 3W9I, respectively) [78,79]. Spreading within the Gram-negatives membranes, RND transporters form a tripartite assembly to give the AcrAB–TolC EP in the case of *E. coli* or MexAB–OprM of *P. aeruginosa* [80]. These transporters are much larger than MFS and are typically composed of approximately 1000 amino acid residues arranged in 12 TM α -helices. RND transporters are organized in trimers, and the substrate efflux is coupled with a proton movement [13]. In recent years, the research around RND transporters has experienced strong progress, thereby shedding light on the mechanisms involved in the efflux and opening the way for a rational identification of EPIs. Good progress has been made especially against *E. coli* and *P. aeruginosa*, where some pyranopyridines strongly potentiated the antibacterial activity of CPX, levofloxacin and piperacillin [81–84]. For one of these derivatives, the co-crystal structure (PDB code: 5ENO) [85] is also available while binding the AcrB subunit of AcrAB–TolC EP of *E. coli*. To date, for some pyranopyridines are ongoing in vivo studies [84]. Another interesting example is shown by a pyridopyrimidine derivative, whose co-crystal structures with AcrB and MexB are available (PDB codes: 3W9H and 3W9J, respectively) [79]. Unfortunately, the best pyridopyrimidine derivative exhibited toxic and pharmacodynamic issues in vivo [86].

3.1. Quinoline Derivatives

One of the first examples regarding quinoline acting as Gram-negative EPIs reported in literature goes back to when Chevalier et al. [87], in 2001, described a series of pyridoquinoline analogues as inhibitors of different EPs in *Enterobacter aerogenes*. All derivatives were tested alone or in combination with CPX (Figure 1) and norfloxacin (NFX—Figure 11) against the wild-type strain ATCC 13048 and its parent, ATCC 13048 p9 (Table 1), harboring a plasmid overexpressing *marA* gene, an activator of EPs expression [88,89], which was found to be 20-fold more resistant to CPX (MIC moved from 0.025 to 0.5 $\mu\text{g}/\text{mL}$). Compounds showed modest MIC values against the wild-type strain (64 $\mu\text{g}/\text{mL}$) that significantly increased against the resistant strains (512–1024 $\mu\text{g}/\text{mL}$), likely resulting from EP substrates. When combined at 16 $\mu\text{g}/\text{mL}$ with CPX or NFX against both strains, compounds 30 and 31 (Figure 12) exhibited a promising synergistic effect with CPX by reducing by 20- and 5-fold, respectively, with its MIC only against ATCC 13048 p9. Surprisingly, only 31 retained a synergistic effect with NFX. EPI activity was demonstrated by the accumulation of labeled NFX in ATCC 13048 p9.

In 2003, Gallo et al. reported a series of quinoline ethers or quinoline thio-ethers synergizing with CAF (Figure 11) against the resistant *E. aerogenes* strain (EA2—Table 1). Among all derivatives, compound 32 (Figure 12) exhibited the best activity, with an MPC₈ of 500 μM (173 $\mu\text{g}/\text{mL}$) (MIC CAF moved from 512 to 64 $\mu\text{g}/\text{mL}$) [90].

In the same year, Mallea et al. reported a series of alkylaminoquinolines as inhibitors of the AcrAB–TolC EP in *E. aerogenes* [91]. Compounds 33 and 34 (Figure 12), with an MIC of 1 mM (314 and 330 $\mu\text{g}/\text{mL}$, respectively) on EA27, emerged as promising compounds by showing a chloramphenicol (CAF) MPC₁₆ of 0.2 and 0.5 mM (63 and 165 $\mu\text{g}/\text{mL}$), respectively, against EA27 strain overexpressing the AcrAB efflux system (Table 1). SAR information highlighted the essential role of some alkylamino chains, such as piperidinoethyl and morpholinopropyl. Indeed, when diethylamino, dimethylamino or di-isopropylamino chains were linked to the aminoquinoline core, there was a significant reduction in the synergistic activity with CAF [91]. The best derivative 33 was also able to increase by the intracellular concentration of radiolabeled CAF in the EA27 strain 3-fold, similarly to PA β N, a known nonspecific Gram-negative EPI [92]. In addition, 33 was evaluated for its ability to decrease MIC values of structurally unrelated antibiotics (CAF, NFX, tetracycline (TET) and cefepime (CEF)—Figure 11) against different *E. aerogenes* strains in which decreasing porins levels were associated with the increasing of MDR. Data showed that compound 33

at 0.2 mM (63 $\mu\text{g}/\text{mL}$) mostly increased the susceptibilities to NFX (8-fold MIC reduction) and CAF (16-fold MIC reduction) when tested against EA27 and EA117 strains (Table 1), highlighting a better synergistic effect than PA β N. From these preliminary results, the class of alkylaminoquinoline seemed to be promising to develop Gram-negative EPIs, but further investigation should be made.

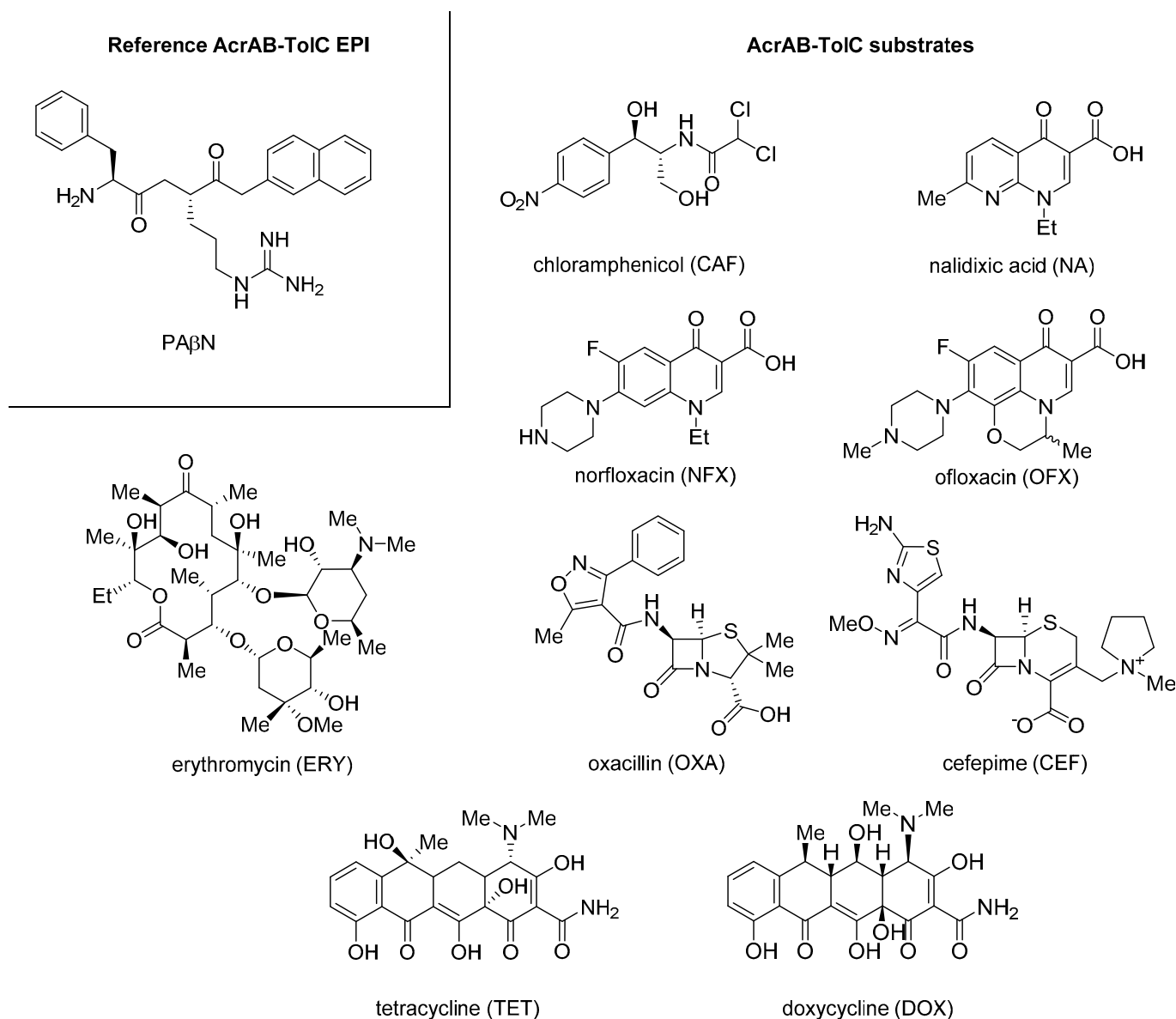


Figure 11. Reference AcrAB–TolC EPI PA β N and AcrAB–TolC substrates chloramphenicol (CAF), nalidixic acid (NA), norfloxacin (NFX), ofloxacin (OFX), oxacillin (OXA), cefepime (CEF), erythromycin (ERY), tetracycline (TET) and doxycycline (DOX).

In 2004, Chevalier et al. described a series of quinolines, with two methyl groups at C-2 and C-8 positions and an ether functionality at C-4 bearing an alkylamino chain, as Gram-negative EPIs [93]. From an initial screening in combination with CAF against EA27, compound 35 (Figure 12—MIC > 10 mM) exhibited the best synergistic activity, with an MPC₈ of 500 μM (135 $\mu\text{g}/\text{mL}$). The synergistic activity of 35 was not related to bacterial membrane disruption, as demonstrated by two different experiments on EA27 strain measuring: (i) potassium leakage and (ii) β -lactamase localization in the periplasm. In addition, it was reported that compound 35 at 1 mM was able to synergize with different antibacterials, such as CAF, NFX and TET, against different strains, such as EA3, synthesizing

channel-altered porins, and EA117 and KP55 (*Klebsiella pneumoniae*), producing very small porin amounts. Interestingly, derivative **35** lost its synergistic activity with CAF and NFX when tested against two different modified EA27 strains where AcrA or TolC were deleted, thus suggesting a specific mechanism of action involving the inhibition of AcrAB–TolC EP. Regarding SAR information, it was evident that only the ethylpyrrolidine chain on the oxygen at the quinoline C-4 position gave the derivative **35** with EPI activity, while other alkylamino chains, though very similar like ethylpiperidine, afforded compounds without this activity.

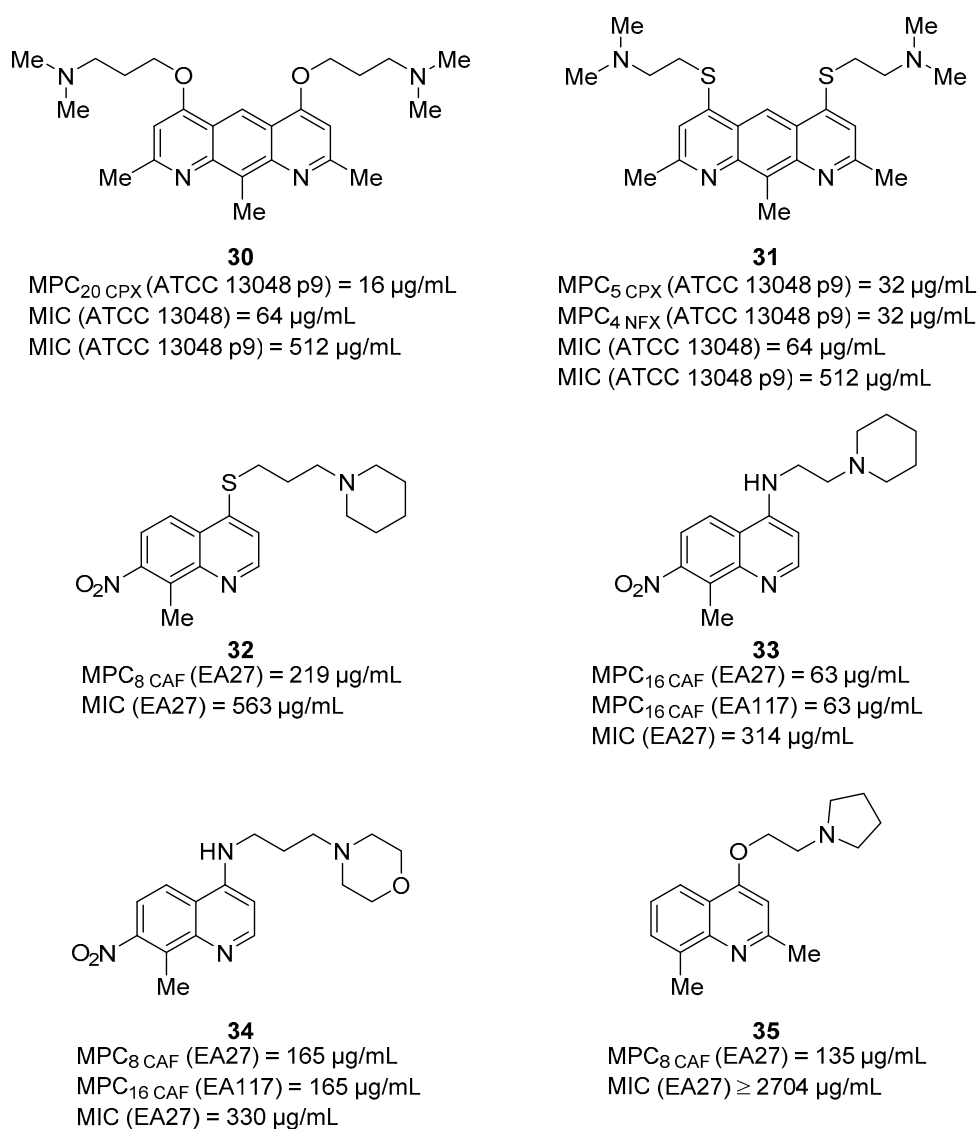


Figure 12. Quinoline derivatives (**30–35**) reported as Gram-negative EPIs.

Few years later, Ghisalberti et al. reported a series of chloroquinolines as potential EPIs towards antibiotic-resistant *E. aerogenes* isolates [94]. Among the six synthesized derivatives, decorated with different alkylamino chains at nitrogen atom at the C-4 position, three compounds (**36–38**—Figure 13) at 0.310 mM (86–95 µg/mL) showed a significant reduction in CAF MIC (by 8-fold) against EA27 and EA5 strains and by 32, 16 and 8-fold, respectively, against the CM-64 strain. In parallel, all three compounds did not show any antibacterial activity on their own and any synergistic effect when tested in combination with CAF against the wild-type *E. aerogenes* ATCC 13048.

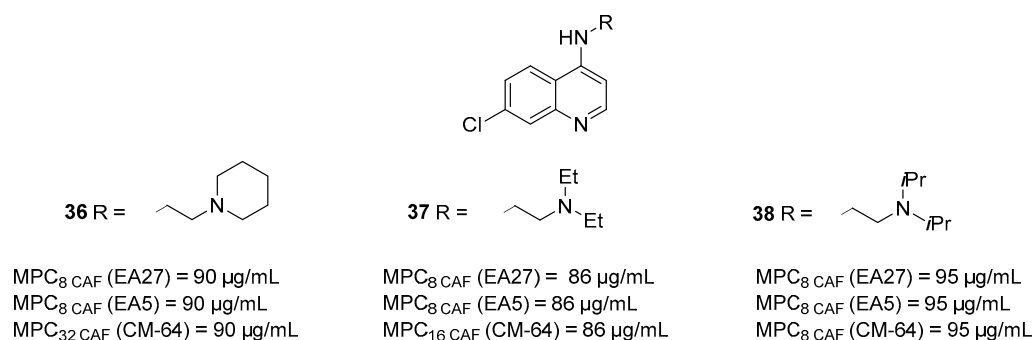


Figure 13. Quinoline derivatives (36–38) reported as Gram-negative EPIs.

In 2016, Machado et al. reported an in-depth study on the role of a previously identified NorA EPI **23** (Figure 7) [64] with a 2-phenylquinoline scaffold as an *E. coli* EPI [95]. During the first step of the study, aimed at excluding any antibacterial activity of **23** against three different *E. coli* strains (the wild-type AG100, the AcrAB-deficient AG100A and AcrAB-overexpressing AG100_{tet}—Table 1), a clear trend was evident. Indeed, **23** showed MIC values of 256 (AG100), 32 (AG100A) and >256 µg/mL (AG100_{tet}), highlighting that the presence of AcrAB significantly influenced the antibacterial activity of **23** and suggesting that it could be considered an AcrAB substrate. However, the synergistic activity of **23** was evaluated in combination with ofloxacin (**OFX**), oxacillin (**OXA**), **TET** and **EtBr** against the three *E. coli* strains. The best results were obtained against AG100_{tet} by the combination of **23** 80 µM (31 µg/mL) with **OFX** (four-fold MIC reduction) and of **23** 40 µM (16 µg/mL) with **TET** (four-fold MIC reduction). In parallel, at the same concentration of **23**, no significant synergism with **OFX** and **TET** was appreciated against AG100 and AG100A strains, thus suggesting an EPI activity dependent on the overexpression of *acrAB*. No synergism was observed between **23** and **OXA** or **EtBr** against all three *E. coli* strains. The EPI activity of **23** was also confirmed through the real-time fluorometry using **EtBr** and determining the relative final fluorescence (RFF) values against AG100, AG100A and AG100_{tet} *E. coli* strains. The results were compared with values obtained for reference compounds (**PAβN** and **CPZ**); compound **23** showed an RFF of 13.1 against the wild-type strain, indicating a strong ability to interfere with **EtBr** efflux compared to **PAβN** and **CPZ**, which showed RFF values of 8.1 and 0.7, respectively. Considering the strain that overexpresses AcrAB–TolC (AG100_{tet}), the quinoline derivative showed an RFF of 5.2, slightly less than **CPZ** but four times higher than **PAβN**, thus suggesting that **23** was able to promote the accumulation of **EtBr** in *E. coli* through the inhibition of the AcrAB. When the effect of **23** on the bacterial membrane potential was evaluated using the BacLight Bacterial Membrane Potential Kit, depolarized cells were over 85%; a value comparable to that was observed for the positive control CCCP (over 95%). Moreover, the possible effects of **23** on the membrane integrity of *E. coli* was evaluated at different concentrations, and no alteration of cell membrane integrity was detected after exposure at 80 µM (31 µg/mL 1/8 MIC) of **23**. Unfortunately, the promising activity of **23** was obtained at concentrations toxic for human monocyte-derived macrophages cells (CC₅₀ = 11 µM/4.24 µg/mL). Information acquired from these preliminary studies displayed **23** as a promising template to develop *E. coli* EPIs, even though some drawbacks should be considered. Indeed, **23** likely was a AcrAB substrate and proved to interfere with PMF, thus indirectly causing the inhibition of the AcrAB–TolC efflux system. Further investigation should be done to define the SAR and improve the safety profile of the compound.

Regarding the SAR information acquired around all quinoline derivatives as Gram-negative EPIs, it was evident that the presence of an alkylamino chain was essential on the heteroatom at C-4 position on the quinoline core. However, unlike quinoline NorA EPIs, the delineated SAR was less clear, with no information about the best side chain to be introduced at the C-4 position. There is no preference for the heteroatom at the C-4 position needed to link the chain with the central scaffold. In addition, the presence of a

NO₂ group at the C-7 position as well as the methyl group at C-8 appear important for the EPI activity of some quinoline derivatives. However, this SAR information mostly came from the works of the research group of Jean-Marie Pagès, and most of them were not identified in the quinoline derivatives reported by Sabatini et al. that lacked both NO₂ and Me groups, while having the phenyl ring at the C-2 position.

3.2. Indole Derivatives

In 2010, Zeng et al. reported a series of indole derivatives as AcrAB–TolC EPIs able to synergize with different antibiotics such as **CAF**, **TET**, erythromycin (**ERY**) and **CPX** against different *E. coli* strains (including the wild-type ATCC 25922 and the resistant YD02—Table 1) [39]. By synergistic assays, compound **39** (Figure 14) at 0.5 mM (88 µg/mL) was able to reduce the **CAF** and **CPX** MICs by 32-fold against the YD02 strain. In parallel, compound **40** (Figure 14) at 0.5 mM (88.0 µg/mL) showed synergistic activities with all the used antibacterials, with MIC reductions ranging from 4 to 32-fold against the YD02 strain. Poor synergistic effects of **39** and **40** with antibacterials were observed against the wild-type strain ATCC 25922 (Table 1). Unfortunately, for the two best compounds, MIC evaluation, checkerboard assays and accumulation assays of antibiotics were not performed.

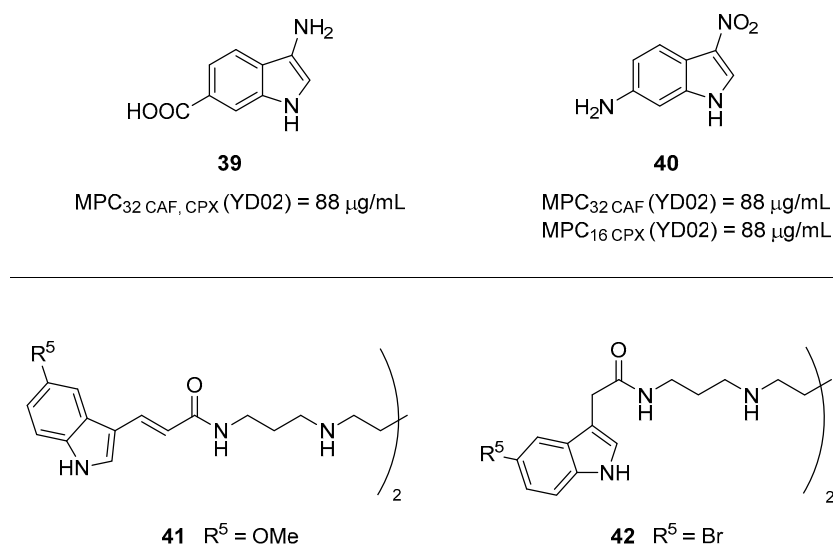


Figure 14. Indole derivatives reported as Gram-negative EPIs.

In 2021, Cadelis et al. reported a series of indole-based spermine derivatives as Gram-negative antibiotic adjuvants [96]. An initial set of synthesized indole derivatives was evaluated for the ability to potentiate doxycycline (**DOX**) activity against the *P. aeruginosa* strain ATCC 27853 (Table 1). The evaluation of the antibiotic adjuvant activity of the best compounds (including **41** and **42**—Figure 14) was next extended towards different Gram-negative bacteria in combination with different antibiotics. In addition, derivative **42** at scalar concentrations was combined with three doses of four different antibiotics against four different bacteria. Results show a significant synergistic effect mainly when combined with (**DOX**) against *P. aeruginosa*, *E. coli* and *K. pneumoniae* and no effect against *A. baumannii*. Less evident synergistic activity of **42** was observed with **ERY**, **CAF** and nalidixic acid (**NA**) against the four bacteria. In-depth studies were performed on derivative **41**, as representative, disclosing its ability to inhibit AcrAB–TolC system in EA289 strain (Table 1) by using the fluorescent probe 1,2'-diNA. However, in further experiments the authors also observed a weak disruption of the *S. aureus* and *P. aeruginosa* membranes and an increase in the membrane permeability of EA289, but only at high concentrations. Interestingly, both compounds **41** and **42** showed high CC₅₀ values against two different cell lines (L6 rat skeletal myoblast cell and HEK-293 human embryonic kidney cells), thus representing promising EPIs.

4. Nontuberculous Mycobacteria (NTM) Efflux Pump Inhibitors

Nontuberculous mycobacteria (NTM) are microorganisms widely distributed in the environment, mostly present in soil and water, including both natural and treated water sources.

The NTM species most frequently encountered in clinical practice are: *M. avium*, *M. intracellulare*, *M. kansasii*, *M. xenopi* and *M. abscessus* [97,98]. Some mycobacteria are able to create communities consisting of several species, such as *M. avium complex* (MAC), which includes *M. avium*, *M. intracellulare* and *M. chimaera*.

Unlike the other microorganisms, NTM are not well known and or studied; therefore, few NTM EPIs are reported in literature.

Only recently, it was shown that NTM EPs are involved in the antimicrobial extrusion and, above all, that their basal expression is very high in these mycobacteria. The classification of EPs in NTM is still in its infancy and, to date, our understanding is based on three recently discovered EPs, MAV_1406 (MFS), MAV_1695 and MAV_3306 (both belonging to ATP-binding cassette) that have been reported to be induced by azithromycin (AZT) exposure and related to the appearance of macrolide-resistant phenotypes [99,100]. Indeed, macrolides, such as clarithromycin (CLA), AZT (Figure 15) and ERY (Figure 11), which are first-line drugs in therapy, are substrates of these pumps.

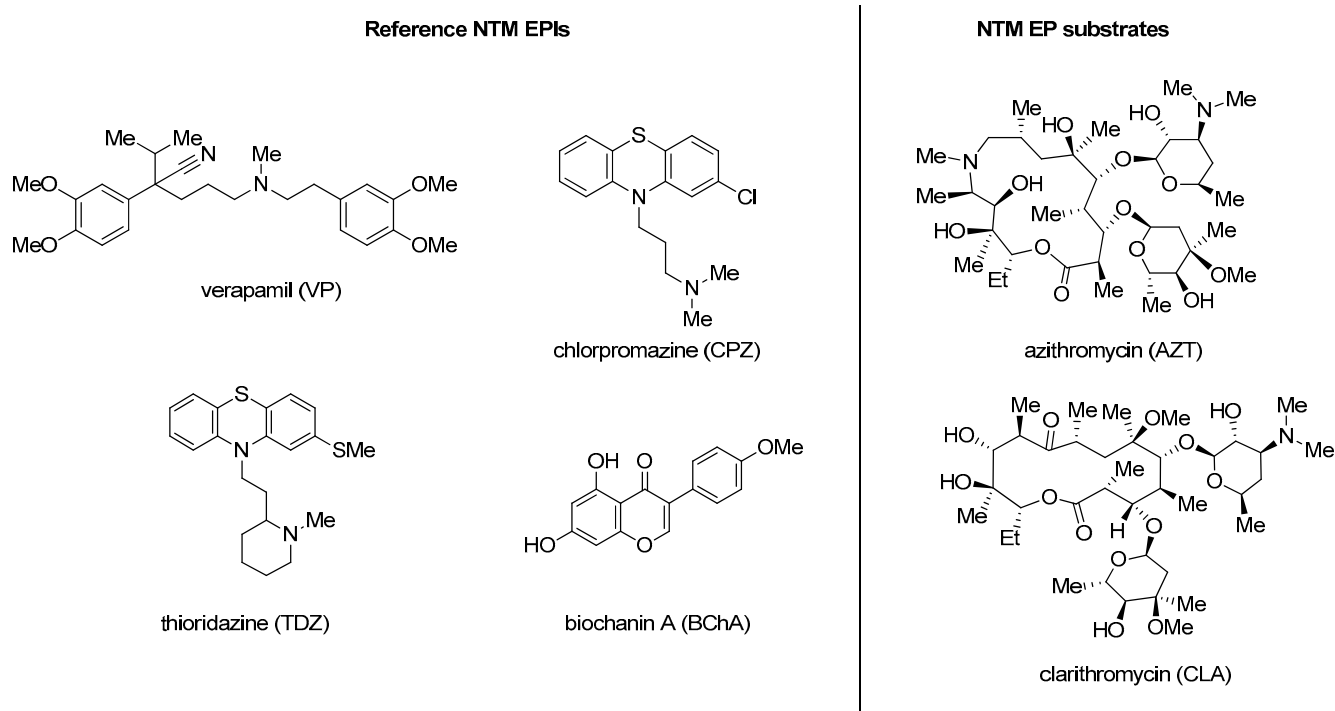


Figure 15. Reference NTM EPIs verapamil (VP), chlorpromazine (CPZ), thioridazine (TDZ) and biochanin A (BChA) and NTM EP substrates azithromycin (AZT) and clarithromycin (CLA).

Studies of Rodriguez et al. have shown that NTM resistance to common antimicrobials was significantly reduced by four non-antibiotic drugs with known EPI activity: verapamil (VP), chlorpromazine (CPZ), thioridazine (TDZ) and biochanin A (BChA) (Figure 15) [100–104].

Quinoline Derivatives

A set of four quinoline derivatives, previously reported as NorA EPIs, was tested to evaluate their ability to: (i) inhibit EtBr efflux, (ii) increase EtBr accumulation and (iii) synergize with CLA against *M. smegmatis* mc² 155 (ATCC700084—Table 1) [43]. The rationale of the initial screening was to identify potential compounds with “broad-spectrum”

EPI activity, likely due to the inhibition of NTM EPs belonging to the MFS family as NorA. Compound **23** (Figure 7) exhibited the best EPI activity towards *M. smegmatis* mc² 155, and thus it was advanced for further investigations against several *M. avium* strains. Through synergistic assays, compound **23** was able to synergize with three antibiotics (**CLA**, **ERY** and **AZT**) against different *M. avium* strains with different characteristics, also including the resistance to macrolides due to the overexpression of EPs. As representative, compound **23** at $\frac{1}{2}$ its MIC (ranging from 32 to 64 $\mu\text{g}/\text{mL}$ depending on the used *M. avium* strain) was able to reduce antibiotic MICs by values > 512 fold. EP inhibition as mechanism of action of **23** was demonstrated by synergistic assays with **EtBr** against all the used *M. avium* strains and also by **EtBr** efflux and accumulation assays against three different *M. avium* strains differing for the expression of EPs. Unfortunately, **23** exhibited high toxicity towards human monocyte-derived macrophages at the concentrations needed to reach its synergistic effect. Two medicinal chemistry works followed the identification of **23** as NTM EPI, leading to the identification of potent compounds acting at concentrations nontoxic for human monocyte-derived macrophages [105,106]. The initial 2-phenylquinoline structure of **23** was optimized to give 3-phenylquinolone analogues that exhibited a more potent EPI activity synergizing at low concentrations with antibiotics against *M. avium* strains. Therefore, the shift of the phenyl moiety at C-3 position and the functionalization of N-1 with alkylamino chains yielding 3-phenylquinolone was beneficial for improving NTM EPI activity, but it was slightly detrimental for NorA EPI activity. Indeed, in a head-to-head comparison between the parent 3-phenylquinolone and 2-phenylquinoline analogues, the former showed a reduced ability to inhibit the **EtBr** efflux on SA-1199B (Table 1) at 50 μM . On the contrary, many 2-phenylquinoline derivatives endowed with potent NorA EPI activity displayed a reduced NTM EPI effect (unpublished data). Taken together, these data suggest a slightly different pharmacophore needed for NorA and NTM EP inhibitions. As a confirmation, the introduction of the OMe group at the C-6 position of 3-phenylquinolone core did not lead to an increase in NTM EPI activity, as previously observed for C-6 OMe 2-phenylquinoline NorA EPIs. On the contrary, at the C-6 position of the 3-phenylquinolone core, a lipophilic moiety was well tolerated, leading to potent and safe NTM EPIs (derivatives **43** and **44**—Figure 16).

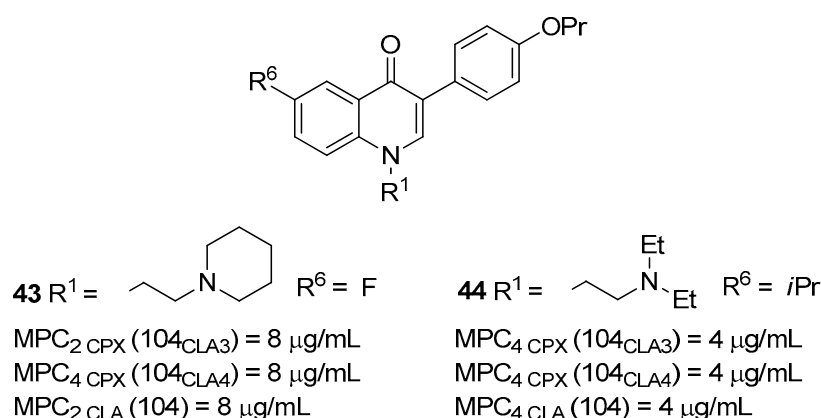


Figure 16. 3-phenylquinolones as NTM EPIs.

Both compounds showed significant synergism with **CLA**, **CPX** and **EtBr** against three different *M. avium* strains. In particular, **44**, at $\frac{1}{32}$ its MIC (4 $\mu\text{g}/\text{mL}$ /8.75 μM), reduced the **CPX** MIC by four-fold against *M. avium* 10₄CLA₃ and 10₄CLA₄ strains and the **CLA** MIC by four-fold against *M. avium* 10₄ strain (Table 1). Inhibition of EPs was demonstrated by **EtBr** efflux and accumulation assays against three *M. avium* strains. Due to its CC₅₀ of 56.32 μM towards human monocyte-derived macrophages, derivative **44** was also tested at 8.75 μM for its activity against an intracellular infection of *M. avium* 10₄ in human monocyte-derived macrophages as alone or in combination with **CLA**. The combination of **CLA** and **44** led to a strong boosting of anti-*M. avium* activity with respect to **CLA** alone.

Interestingly, although tested at $1/32$ its MIC, **44** also exhibited a similar anti-*M. avium* activity when tested alone, thus suggesting a potential and essential role of the NTM EPs during intracellular infections.

5. Conclusions

In this review, we collected all data regarding indole and quinoline derivatives reported in literature as microbial EPs. When possible, SAR information has been highlighted and discussed to generate a sort of comprehensive SAR around each scaffold with the aim to help the future research of new microbial EPs.

Regarding the collected information, we observed that most of the compounds (belonging to the quinoline and indole classes) have been reported as NorA EPs, thus synergizing with the fluoroquinolone CPX against different strains of *S. aureus*. Accordingly, the best results in terms of EP inhibition have been obtained against NorA, with some compounds able to synergize with CPX at low concentrations as 0.78 $\mu\text{g}/\text{mL}$ [69]. Interestingly, these findings appear in contrast with those observed for EPs of Gram-negative bacteria. Indeed, although quinoline and indole derivatives showed significant synergism, though often at only high concentrations, the research of Gram-negative EPs has led to some derivatives reached in vivo studies [86,107]. Accordingly, for AcrAB–TolC (*E. coli*) [108] and MexAB–OprM (*P. aeruginosa*) [109], both EPs belonging to the RND family, there are crystal structures of the whole complexes and, for AcrB and MexB 3D structures in complex with EPs have been also reported [79,85], thus allowing for future structure-based drug design approaches.

Therefore, quinoline and indole derivatives would appear to be suitable scaffolds to obtain potent NorA EPs synergizing with antibiotics at very low concentrations, while representing only tool compounds in the field of Gram-negative EPs. Of note, it is evident that most of quinoline EPs need an alkylamino chain to better synergize with antibiotics, in contrast to indole EPs, where only few derivatives have been reported with basic side chains. Finally, research for NTM EPs is still in its infancy and, to date, only few molecules have been described in literature. Accordingly, the delineation of a SAR appears complicated, but the few quinoline and quinolone derivatives showing EPI activity can represent a good starting point for future research also aimed at identifying the role of EPs during intracellular infections.

Supplementary Materials: The following are available online. Table S1: Chemical name and structure of the described EPI compounds.

Author Contributions: Conceptualization, G.C., T.F. and S.S.; writing—original draft preparation, G.C. and T.F.; writing—review and editing, T.F. and S.S.; supervision, S.S. All authors have read and agreed to the published version of the manuscript.

Funding: This research received no external funding.

Institutional Review Board Statement: Not applicable.

Informed Consent Statement: Not applicable.

Conflicts of Interest: The authors declare no conflict of interest.

Abbreviations

ABC: ATP-binding cassette; AMR, antimicrobial resistance; ARB, antimicrobial resistance breaker; AZT, azithromycin; BChA, biochanin A; CAF, chloramphenicol; CEF, cefepime; CLA, clarithromycin; CPX, ciprofloxacin; CPZ, chlorpromazine; DOX, doxycycline; EP, efflux pump; EPI, efflux pump inhibitor; ERY, erythromycin; EtBr, ethidium bromide; HCT116, human colon tumor; KB, keratin-forming tumor HeLa; HePG2, human liver epithelial; MAC, *M. avium* complex; MATE, multidrug and toxic compound extrusion; MCF7, breast cancer; MCF7R, breast carcinoma; MCR5, human lung fibroblast; MFS, major facilitator superfamily; MIC, minimal inhibitory concentration; MPC, minimal potentiating concentration; MRSA, methicillin resistant *Staphylococcus aureus*; NFX, nor-

floxacin; NTM, nontuberculous mycobacteria; OFX, ofloxacin; OM, outer membrane; OXA, oxacillin; PACE, proteobacterial antimicrobial compound efflux; RES, reserpine; RFF, relative final fluorescence; RND, resistance–nodulation–cell division; SAR, structure-activity relationship; SMR, small multidrug resistance; TDZ, thioridazine; TET, tetracycline; THP1, human monocytic cell line; VP, verapamil.

References

1. World Health Organization. *Global Antimicrobial Resistance and Use Surveillance System (GLASS) Report: 2021*; World Health Organization: Geneva, Switzerland, 2021.
2. Miethke, M.; Pieroni, M.; Weber, T.; Brönstrup, M.; Hammann, P.; Halby, L.; Arimondo, P.B.; Glaser, P.; Aigle, B.; Bode, H.B.; et al. Towards the sustainable discovery and development of new antibiotics. *Nat. Rev. Chem.* **2021**, *5*, 726–749. [[CrossRef](#)] [[PubMed](#)]
3. Kyriakides, S. EU Action on Antimicrobial Resistance | Public Health. 2016. Available online: <https://ec.europa.eu/health/antimicrobial-resistance/eu-action-on-antimicrobial-resistance.it> (accessed on 16 November 2021).
4. Melander, R.J.; Melander, C. The Challenge of Overcoming Antibiotic Resistance: An Adjuvant Approach? *ACS Infect. Dis.* **2017**, *3*, 559–563. [[CrossRef](#)] [[PubMed](#)]
5. Brown, D. Antibiotic resistance breakers: Can repurposed drugs fill the antibiotic discovery void? *Nat. Rev. Drug Discov.* **2015**, *14*, 821–832. [[CrossRef](#)]
6. Wright, G.D. Antibiotic Adjuvants: Rescuing Antibiotics from Resistance. *Trends Microbiol.* **2016**, *24*, 862–871. [[CrossRef](#)] [[PubMed](#)]
7. Martins, M.; Dastidar, S.G.; Fanning, S.; Kristiansen, J.E.; Molnar, J.; Pagès, J.-M.; Schelz, Z.; Spengler, G.; Viveiros, M.; Amaral, L. Potential role of non-antibiotics (helper compounds) in the treatment of multidrug-resistant Gram-negative infections: Mechanisms for their direct and indirect activities. *Int. J. Antimicrob. Agents* **2008**, *31*, 198–208. [[CrossRef](#)] [[PubMed](#)]
8. Rasko, D.A.; Sperandio, V. Anti-virulence strategies to combat bacteria-mediated disease. *Nat. Rev. Drug Discov.* **2010**, *9*, 117–128. [[CrossRef](#)] [[PubMed](#)]
9. Rampioni, G.; Pillai, C.R.; Longo, F.; Bondi, R.; Baldelli, V.; Messina, M.; Imperi, F.; Visca, P.; Leoni, L. Effect of efflux pump inhibition on *Pseudomonas aeruginosa* transcriptome and virulence. *Sci. Rep.* **2017**, *7*, 11392. [[CrossRef](#)]
10. Vermote, A.; Van Calenbergh, S. Small-Molecule Potentiators for Conventional Antibiotics against *Staphylococcus aureus*. *ACS Infect. Dis.* **2017**, *3*, 780–796. [[CrossRef](#)]
11. González-Bello, C.; Rodríguez, D.; Pernas, M.; Rodríguez, Á.; Colchón, E. β -Lactamase Inhibitors to Restore the Efficacy of Antibiotics against Superbugs. *J. Med. Chem.* **2020**, *63*, 1859–1881. [[CrossRef](#)] [[PubMed](#)]
12. Piddock, L.J.V. Multidrug-resistance efflux pumps—Not just for resistance. *Nat. Rev. Microbiol.* **2006**, *4*, 629–636. [[CrossRef](#)] [[PubMed](#)]
13. Du, D.; Wang-Kan, X.; Neuberger, A.; van Veen, H.W.; Pos, K.M.; Piddock, L.J.V.; Luisi, B.F. Multidrug efflux pumps: Structure, function and regulation. *Nat. Rev. Microbiol.* **2018**, *16*, 523–539. [[CrossRef](#)]
14. Saier, M.H.; Tran, C.V.; Barabote, R.D. TCDB: The Transporter Classification Database for membrane transport protein analyses and information. *Nucleic Acids Res.* **2006**, *34*, 181–186. [[CrossRef](#)] [[PubMed](#)]
15. Schindler, B.D.; Kaatz, G.W. Multidrug efflux pumps of Gram-positive bacteria. *Drug Resist. Updates* **2016**, *27*, 1–13. [[CrossRef](#)] [[PubMed](#)]
16. Venter, H.; Mowla, R.; Ohene-Agyei, T.; Ma, S. RND-type drug efflux pumps from Gram-negative bacteria: Molecular mechanism and inhibition. *Front. Microbiol.* **2015**, *6*, 377. [[CrossRef](#)] [[PubMed](#)]
17. Lomovskaya, O.; Bostian, K.A. Practical applications and feasibility of efflux pump inhibitors in the clinic—A vision for applied use. *Biochem. Pharmacol.* **2006**, *71*, 910–918. [[CrossRef](#)]
18. Piddock, L.J.V. Understanding the basis of antibiotic resistance: A platform for drug discovery. *Microbiology* **2014**, *160*, 2366–2373. [[CrossRef](#)]
19. Ricci, V.; Tzakas, P.; Buckley, A.; Coldham, N.C.; Piddock, L.J.V. Ciprofloxacin-resistant *Salmonella enterica* serovar typhimurium strains are difficult to select in the absence of AcrB and TolC. *Antimicrob. Agents Chemother.* **2006**, *50*, 38–42. [[CrossRef](#)]
20. Zhang, Q.; Lambert, G.; Liao, D.; Kim, H.; Robin, K.; Tung, C.K.; Pourmand, N.; Austin, R.H. Acceleration of emergence of bacterial antibiotic resistance in connected microenvironments. *Science* **2011**, *333*, 1764–1767. [[CrossRef](#)] [[PubMed](#)]
21. Baugh, S.; Phillips, C.R.; Ekanayaka, A.S.; Piddock, L.J.V.; Webber, M.A. Inhibition of multidrug efflux as a strategy to prevent biofilm formation. *J. Antimicrob. Chemother.* **2014**, *69*, 673–681. [[CrossRef](#)]
22. Kvist, M.; Hancock, V.; Klemm, P. Inactivation of efflux pumps abolishes bacterial biofilm formation. *Appl. Environ. Microbiol.* **2008**, *74*, 7376–7382. [[CrossRef](#)]
23. Sabatini, S.; Piccioni, M.; Felicetti, T.; De Marco, S.; Manfroni, G.; Pagiotti, R.; Nocchetti, M.; Cecchetti, V.; Pietrella, D. Investigation on the effect of known potent: *S. aureus* NorA efflux pump inhibitors on the staphylococcal biofilm formation. *RSC Adv.* **2017**, *7*, 37007–37014. [[CrossRef](#)]
24. Schillaci, D.; Spanò, V.; Parrino, B.; Carbone, A.; Montalbano, A.; Barraja, P.; Diana, P.; Cirrincione, G.; Cascioferro, S. Pharmaceutical Approaches to Target Antibiotic Resistance Mechanisms. *J. Med. Chem.* **2017**, *60*, 8268–8297. [[CrossRef](#)]
25. Lamut, A.; Peterlin Mašič, L.; Kikelj, D.; Tomašič, T. Efflux pump inhibitors of clinically relevant multidrug resistant bacteria. *Med. Res. Rev.* **2019**, *39*, 2460–2504. [[CrossRef](#)]

26. Martinez, J.L.; Sánchez, M.B.; Martínez-Solano, L.; Hernandez, A.; Garmendia, L.; Fajardo, A.; Alvarez-Ortega, C. Functional role of bacterial multidrug efflux pumps in microbial natural ecosystems. *FEMS Microbiol. Rev.* **2009**, *33*, 430–449. [[CrossRef](#)]
27. Kaatz, G.W.; Seo, S.M.; Ruble, C.A. Efflux-mediated fluoroquinolone resistance in *Staphylococcus aureus*. *Antimicrob. Agents Chemother.* **1993**, *37*, 1086–1094. [[CrossRef](#)]
28. Kaatz, G.W.; Seo, S.M.; Ruble, C.A. Mechanisms of Fluoroquinolone Resistance in *Staphylococcus aureus*. *J. Infect. Dis.* **1991**, *163*, 1080–1086. [[CrossRef](#)]
29. Novick, R. Properties of a cryptic high-frequency transducing phage in *Staphylococcus aureus*. *Virology* **1967**, *33*, 155–166. [[CrossRef](#)]
30. Price, C.T.D.; Kaatz, G.W.; Gustafson, J.E. The multidrug efflux pump NorA is not required for salicylate-induced reduction in drug accumulation by *Staphylococcus aureus*. *Int. J. Antimicrob. Agents* **2002**, *20*, 206–213. [[CrossRef](#)]
31. Tegos, G.; Stermitz, F.R.; Lomovskaya, O.; Lewis, K. Multidrug Pump Inhibitors Uncover Remarkable Activity of Plant Antimicrobials. *Antimicrob. Agents Chemother.* **2002**, *46*, 3133. [[CrossRef](#)]
32. Kaatz, G.W.; Seo, S.M. Inducible NorA-Mediated Multidrug Resistance in *Staphylococcus aureus*. *Antimicrob. Agents Chemother.* **1995**, *39*, 2650–2655. [[CrossRef](#)]
33. Gambino, L.; Gracheck, S.J.; Miller, P.F. Overexpression of the MarA positive regulator is sufficient to confer multiple antibiotic resistance in *Escherichia coli*. *J. Bacteriol.* **1993**, *175*, 2888–2894. [[CrossRef](#)]
34. Mallea, M.; Chevalier, J.; Bornet, C.; Eyraud, A.; Davin-Regli, A.; Bollet, C.; Pages, J.M. Porin alteration and active efflux: Two in vivo drug resistance strategies used by *Enterobacter aerogenes*. *Microbiology* **1998**, *144*, 3003–3009. [[CrossRef](#)]
35. Ghisalberti, D.; Masi, M.; Pagès, J.M.; Chevalier, J. Chloramphenicol and expression of multidrug efflux pump in *Enterobacter aerogenes*. *Biochem. Biophys. Res. Commun.* **2005**, *328*, 1113–1118. [[CrossRef](#)]
36. Pradel, E.; Pagès, J.M. The AcrAB–TolC efflux pump contributes to multidrug resistance in the nosocomial pathogen *Enterobacter aerogenes*. *Antimicrob. Agents Chemother.* **2002**, *46*, 2640–2643. [[CrossRef](#)]
37. Ito, H.; Fukuda, Y.; Murata, K.; Kimura, A. Transformation of intact yeast cells treated with alkali cations. *J. Bacteriol.* **1983**, *153*, 163. [[CrossRef](#)] [[PubMed](#)]
38. Viveiros, M.; Jesus, A.; Brito, M.; Leandro, C.; Martins, M.; Ordway, D.; Molnar, A.M.; Molnar, J.; Amaral, L. Inducement and Reversal of Tetracycline Resistance in *Escherichia coli* K-12 and Expression of Proton Gradient-Dependent Multidrug Efflux Pump Genes. *Antimicrob. Agents Chemother.* **2005**, *49*, 3578. [[CrossRef](#)]
39. Zeng, B.; Wang, H.; Zou, L.; Zhang, A.; Yang, X.; Guan, Z. Evaluation and Target Validation of Indole Derivatives as Inhibitors of the AcrAB–TolC Efflux Pump. *Biosci. Biotechnol. Biochem.* **2010**, *74*, 2237–2241. [[CrossRef](#)]
40. Chevalier, J.; Pagès, J.M.; Eyraud, A.; Mallea, M. Membrane Permeability Modifications Are Involved in Antibiotic Resistance in *Klebsiella pneumoniae*. *Biochem. Biophys. Res. Commun.* **2000**, *274*, 496–499. [[CrossRef](#)] [[PubMed](#)]
41. Snapper, S.B.; Melton, R.E.; Mustafa, S.; Kieser, T.; Jacobs, W.R. Isolation and characterization of efficient plasmid transformation mutants of *Mycobacterium smegmatis*. *Mol. Microbiol.* **1990**, *4*, 1911–1919. [[CrossRef](#)]
42. Horan, K.L.; Freeman, R.; Weigel, K.; Semret, M.; Pfaller, S.; Covert, T.C.; van Soolingen, D.; Leao, S.C.; Behr, M.A.; Cangelosi, G.A. Isolation of the genome sequence strain *Mycobacterium avium* 104 from multiple patients over a 17-year period. *J. Clin. Microbiol.* **2006**, *44*, 783–789. [[CrossRef](#)]
43. Machado, D.; Cannalire, R.; Santos Costa, S.; Manfroni, G.; Tabarrini, O.; Cecchetti, V.; Couto, I.; Viveiros, M.; Sabatini, S. Boosting Effect of 2-Phenylquinoline Efflux Inhibitors in Combination with Macrolides against *Mycobacterium smegmatis* and *Mycobacterium avium*. *ACS Infect. Dis.* **2016**, *1*, 593–603. [[CrossRef](#)] [[PubMed](#)]
44. Boucher, H.W.; Talbot, G.H.; Bradley, J.S.; Edwards, J.E.; Gilbert, D.; Rice, L.B.; Scheld, M.; Spellberg, B.; Bartlett, J. Bad Bugs, No Drugs: No ESKAPE! An Update from the Infectious Diseases Society of America. *Clin. Infect. Dis.* **2009**, *48*, 1–12. [[CrossRef](#)] [[PubMed](#)]
45. Costa, S.S.; Viveiros, M.; Amaral, L.; Couto, I. Multidrug Efflux Pumps in *Staphylococcus aureus*: An Update. *Open Microbiol. J.* **2013**, *7*, 59–71. [[CrossRef](#)] [[PubMed](#)]
46. Jang, S. Multidrug efflux pumps in *Staphylococcus aureus* and their clinical implications. *J. Microbiol.* **2016**, *54*, 1–8. [[CrossRef](#)]
47. Ubukata, K.; Itoh-Yamashita, N.; Konno, M. Cloning and expression of the norA gene for fluoroquinolone resistance in *Staphylococcus aureus*. *Antimicrob. Agents Chemother.* **1989**, *33*, 1535–1539. [[CrossRef](#)] [[PubMed](#)]
48. Yoshida, H.; Bogaki, M.; Nakamura, S.; Ubukata, K.; Konno, M. Nucleotide sequence and characterization of the *Staphylococcus aureus* norA gene, which confers resistance to quinolones. *J. Bacteriol.* **1990**, *172*, 6942–6949. [[CrossRef](#)] [[PubMed](#)]
49. Bhaskar, B.V.; Chandra Babu, T.M.; Reddy, N.V.; Rajendra, W. Homology modeling, molecular dynamics, and virtual screening of NorA efflux pump inhibitors of *Staphylococcus aureus*. *Drug Des. Devel. Ther.* **2016**, *10*, 3237–3252. [[CrossRef](#)] [[PubMed](#)]
50. Tintino, S.R.; de Souza, V.C.A.; da Silva, J.M.A.; Oliveira-Tintino, C.D.; Pereira, P.S.; Leal-Balbino, T.C.; Pereira-Neves, A.; Siqueira-Junior, J.P.; da Costa, J.G.M.; Rodrigues, F.F.G.; et al. Effect of Vitamin K3 Inhibiting the Function of NorA Efflux Pump and Its Gene Expression on *Staphylococcus aureus*. *Membranes* **2020**, *10*, 130. [[CrossRef](#)] [[PubMed](#)]
51. Palazzotti, D.; Bissaro, M.; Bolcato, G.; Astolfi, A.; Felicetti, T.; Sabatini, S.; Sturlese, M.; Cecchetti, V.; Barreca, M.L.; Moro, S. Deciphering the Molecular Recognition Mechanism of Multidrug Resistance *Staphylococcus aureus* NorA Efflux Pump Using a Supervised Molecular Dynamics Approach. *Int. J. Mol. Sci.* **2019**, *20*, 4041. [[CrossRef](#)] [[PubMed](#)]
52. Markham, P.N.; Westhaus, E.; Klyachko, K.; Johnson, M.E.; Neyfakh, A.A. Multiple novel inhibitors of the NorA multidrug transporter of *Staphylococcus aureus*. *Antimicrob. Agents Chemother.* **1999**, *43*, 2404–2408. [[CrossRef](#)]

53. Neyfakh, A.A.; Borsch, C.M.; Kaatz, G.W. Fluoroquinolone resistance protein NorA of *Staphylococcus aureus* is a multidrug efflux transporter. *Antimicrob. Agents Chemother.* **1993**, *37*, 128–129. [[CrossRef](#)] [[PubMed](#)]
54. Ahmed, M.; Lyass, L.; Markham, P.N.; Taylor, S.S.; Vazquez-Laslop, N.; Neyfakh, A.A. Two highly similar multidrug transporters of *Bacillus subtilis* whose expression is differentially regulated. *J. Bacteriol.* **1995**, *177*, 3904–3910. [[CrossRef](#)] [[PubMed](#)]
55. Samosorn, S.; Bremner, J.; Ball, A.; Lewis, K. Synthesis of functionalized 2-aryl-5-nitro-1H-indoles and their activity as bacterial NorA efflux pump inhibitors. *Bioorg. Med. Chem.* **2006**, *14*, 857–865. [[CrossRef](#)] [[PubMed](#)]
56. dit Chabert, J.F.; Marquez, B.; Neville, L.; Joucla, L.; Broussous, S.; Bouhours, P.; David, E.; Pellet-Rostaing, S.; Marquet, B.; Moreau, N.; et al. Synthesis and evaluation of new arylbenzo[b]thiophene and diarylthiophene derivatives as inhibitors of the NorA multidrug transporter of *Staphylococcus aureus*. *Bioorg. Med. Chem.* **2007**, *15*, 4482–4497. [[CrossRef](#)]
57. Ambrus, J.I.; Kelso, M.J.; Bremner, J.B.; Ball, A.R.; Casadei, G.; Lewis, K. Structure-activity relationships of 2-aryl-1H-indole inhibitors of the NorA efflux pump in *Staphylococcus aureus*. *Bioorg. Med. Chem. Lett.* **2008**, *18*, 4294–4297. [[CrossRef](#)] [[PubMed](#)]
58. Hequet, A.; Burchak, O.N.; Jeanty, M.; Guinchard, X.; Le Pihive, E.; Maigre, L.; Bouhours, P.; Schneider, D.; Maurin, M.; Paris, J.M.; et al. 1-(1H-indol-3-yl)ethanamine derivatives as potent *Staphylococcus aureus* NorA efflux pump inhibitors. *ChemMedChem* **2014**, *9*, 1534–1545. [[CrossRef](#)]
59. Burchak, O.N.; Le Pihive, E.; Maigre, L.; Guinchard, X.; Bouhours, P.; Jolival, C.; Schneider, D.; Maurin, M.; Giglione, C.; Meinel, T.; et al. Synthesis and evaluation of 1-(1H-indol-3-yl)ethanamine derivatives as new antibacterial agents. *Bioorg. Med. Chem.* **2011**, *19*, 3204–3215. [[CrossRef](#)]
60. Liger, F.; Pellet-Rostaing, S.; Popowycz, F.; Lemaire, M. Bromination of 3-substituted benzo[b]thiophenes: Access to Raloxifen intermediate. *Tetrahedron Lett.* **2011**, *52*, 3736–3739. [[CrossRef](#)]
61. Liger, F.; Bouhours, P.; Ganem-Elbaz, C.; Jolival, C.; Pellet-Rostaing, S.; Popowycz, F.; Paris, J.-M.; Lemaire, M. C2 Arylated Benzo[b]thiophene Derivatives as *Staphylococcus aureus* NorA Efflux Pump Inhibitors. *ChemMedChem* **2016**, *11*, 320–330. [[CrossRef](#)]
62. Lepri, S.; Buonerba, F.; Goracci, L.; Velilla, I.; Ruzziconi, R.; Schindler, B.D.; Seo, S.M.; Kaatz, G.W.; Cruciani, G. Indole Based Weapons to Fight Antibiotic Resistance: A Structure-Activity Relationship Study. *J. Med. Chem.* **2016**, *59*, 867–891. [[CrossRef](#)] [[PubMed](#)]
63. Baroni, M.; Cruciani, G.; Sciabola, S.; Perruccio, F.; Mason, J.S. A Common Reference Framework for Analyzing/Comparing Proteins and Ligands. Fingerprints for Ligands And Proteins (FLAP): Theory and Application. *J. Chem. Inf. Model.* **2007**, *47*, 279–294. [[CrossRef](#)]
64. Sabatini, S.; Gosetto, F.; Iraci, N.; Barreca, M.L.; Massari, S.; Sancineto, L.; Manfroni, G.; Tabarrini, O.; Dimovska, M.; Kaatz, G.W.; et al. Re-evolution of the 2-phenylquinolines: Ligand-based design, synthesis, and biological evaluation of a potent new class of *Staphylococcus aureus* NorA efflux pump inhibitors to combat antimicrobial resistance. *J. Med. Chem.* **2013**, *56*, 4975–4989. [[CrossRef](#)]
65. Buonerba, F.; Lepri, S.; Goracci, L.; Schindler, B.D.; Seo, S.M.; Kaatz, G.W.; Cruciani, G. Improved Potency of Indole-Based NorA Efflux Pump Inhibitors: From Serendipity toward Rational Design and Development. *J. Med. Chem.* **2017**, *60*, 517–523. [[CrossRef](#)] [[PubMed](#)]
66. Schindler, B.D.; Jacinto, P.; Kaatz, G.W. Inhibition of drug efflux pumps in *Staphylococcus aureus*: Current status of potentiating existing antibiotics. *Future Microbiol.* **2013**, *8*, 491–507. [[CrossRef](#)] [[PubMed](#)]
67. Sabatini, S.; Gosetto, F.; Manfroni, G.; Tabarrini, O.; Kaatz, G.W.; Patel, D.; Cecchetti, V. Evolution from a Natural Flavones Nucleus to Obtain 2-(4-Propoxyphenyl)quinoline Derivatives As Potent Inhibitors of the *S. aureus* NorA Efflux Pump. *J. Med. Chem.* **2011**, *54*, 5722–5736. [[CrossRef](#)] [[PubMed](#)]
68. Zloh, M.; Gibbons, S. Molecular Similarity of MDR Inhibitors. *Int. J. Mol. Sci.* **2004**, *5*, 37–47. [[CrossRef](#)]
69. Felicetti, T.; Cannalire, R.; Pietrella, D.; Latacz, G.; Lubelska, A.; Manfroni, G.; Barreca, M.L.; Massari, S.; Tabarrini, O.; Kieć-Kononowicz, K.; et al. 2-Phenylquinoline *S. aureus* NorA efflux pump inhibitors: Evaluation of the importance of methoxy group introduction. *J. Med. Chem.* **2018**, *61*, 7827–7848. [[CrossRef](#)] [[PubMed](#)]
70. Felicetti, T.; Cannalire, R.; Nizi, M.G.; Tabarrini, O.; Massari, S.; Barreca, M.L.; Manfroni, G.; Schindler, B.D.; Cecchetti, V.; Kaatz, G.W.; et al. Studies on 2-phenylquinoline *Staphylococcus aureus* NorA efflux pump inhibitors: New insights on the C-6 position. *Eur. J. Med. Chem.* **2018**, *155*, 428–433. [[CrossRef](#)]
71. Felicetti, T.; Mangiaterra, G.; Cannalire, R.; Cedrarò, N.; Pietrella, D.; Astolfi, A.; Massari, S.; Tabarrini, O.; Manfroni, G.; Barreca, M.L.; et al. C-2 phenyl replacements to obtain potent quinoline-based *Staphylococcus aureus* NorA inhibitors. *J. Enzym. Inhib. Med. Chem.* **2020**, *35*, 584–597. [[CrossRef](#)]
72. Cannalire, R.; Mangiaterra, G.; Felicetti, T.; Astolfi, A.; Cedrarò, N.; Massari, S.; Manfroni, G.; Tabarrini, O.; Vaiasicca, S.; Barreca, M.L.; et al. Structural Modifications of the Quinolin-4-yloxy Core to Obtain New *Staphylococcus aureus* NorA Inhibitors. *Int. J. Mol. Sci.* **2020**, *21*, 7037. [[CrossRef](#)]
73. Cedrarò, N.; Cannalire, R.; Astolfi, A.; Mangiaterra, G.; Felicetti, T.; Vaiasicca, S.; Cernicchi, G.; Massari, S.; Manfroni, G.; Tabarrini, O.; et al. From Quinoline to Quinazoline-Based *S. aureus* NorA Efflux Pump Inhibitors by Coupling a Focused Scaffold Hopping Approach and a Pharmacophore Search. *ChemMedChem* **2021**, *16*, 3044–3059. [[CrossRef](#)] [[PubMed](#)]
74. Astolfi, A.; Felicetti, T.; Iraci, N.; Manfroni, G.; Massari, S.; Pietrella, D.; Tabarrini, O.; Kaatz, G.W.; Barreca, M.L.; Sabatini, S.; et al. Pharmacophore-based repositioning of approved drugs as novel *Staphylococcus aureus* NorA efflux pump inhibitors. *J. Med. Chem.* **2017**, *60*, 1598–1604. [[CrossRef](#)] [[PubMed](#)]

75. Silhavy, T.J.; Kahne, D.; Walker, S. The Bacterial Cell Envelope. *Cold Spring Harb. Perspect. Biol.* **2010**, *2*, a000414. [[CrossRef](#)] [[PubMed](#)]
76. Delcour, A.H. Outer Membrane Permeability and Antibiotic Resistance. *Biochim. Biophys. Acta* **2009**, *1794*, 808. [[CrossRef](#)]
77. Breijyeh, Z.; Jubeh, B.; Karaman, R. Resistance of Gram-Negative Bacteria to Current Antibacterial Agents and Approaches to Resolve It. *Molecules* **2020**, *25*, 1340. [[CrossRef](#)] [[PubMed](#)]
78. Murakami, S.; Nakashima, R.; Yamashita, E.; Yamaguchi, A. Crystal structure of bacterial multidrug efflux transporter AcrB. *Nature* **2002**, *419*, 587–593. [[CrossRef](#)]
79. Nakashima, R.; Sakurai, K.; Yamasaki, S.; Hayashi, K.; Nagata, C.; Hoshino, K.; Onodera, Y.; Nishino, K.; Yamaguchi, A. Structural basis for the inhibition of bacterial multidrug exporters. *Nature* **2013**, *500*, 102–106. [[CrossRef](#)] [[PubMed](#)]
80. Blair, J.M.A.; Richmond, G.E.; Piddock, V.L.J. Multidrug efflux pumps in Gram-negative bacteria and their role in antibiotic resistance. *Future Microbiol.* **2014**, *9*, 1165–1177. [[CrossRef](#)] [[PubMed](#)]
81. Opperman, T.J.; Kwasny, S.M.; Kim, H.S.; Nguyen, S.T.; Houseweart, C.; D’Souza, S.; Walker, G.C.; Peet, N.P.; Nikaido, H.; Bowlin, T.L. Characterization of a novel pyranopyridine inhibitor of the AcrAB efflux pump of *Escherichia coli*. *Antimicrob. Agents Chemother.* **2014**, *58*, 722–733. [[CrossRef](#)] [[PubMed](#)]
82. Vargiu, A.V.; Ruggerone, P.; Opperman, T.J.; Nguyen, S.T.; Nikaido, H. Molecular mechanism of MBX2319 inhibition of *Escherichia coli* AcrB multidrug efflux pump and comparison with other inhibitors. *Antimicrob. Agents Chemother.* **2014**, *58*, 6224–6234. [[CrossRef](#)] [[PubMed](#)]
83. Nguyen, S.T.; Kwasny, S.M.; Ding, X.; Cardinale, S.C.; McCarthy, C.T.; Kim, H.-S.; Nikaido, H.; Peet, N.P.; Williams, J.D.; Bowlin, T.L.; et al. Structure–activity relationships of a novel pyranopyridine series of Gram-negative bacterial efflux pump inhibitors. *Bioorg. Med. Chem.* **2015**, *23*, 2024–2034. [[CrossRef](#)] [[PubMed](#)]
84. Aron, Z.; Opperman, T.J.; Pucci, M.J.; Dougherty, T.J. Optimization of a novel series of pyranopyridine RND efflux pump inhibitors. *Curr. Opin. Microbiol.* **2016**, *33*, 1–6. [[CrossRef](#)]
85. Sjuts, H.; Vargiu, A.V.; Kwasny, S.M.; Nguyen, S.T.; Kim, H.-S.; Ding, X.; Ornik, A.R.; Ruggerone, P.; Bowlin, T.L.; Nikaido, H.; et al. Molecular basis for inhibition of AcrB multidrug efflux pump by novel and powerful pyranopyridine derivatives. *Proc. Natl. Acad. Sci. USA* **2016**, *113*, 3509–3514. [[CrossRef](#)] [[PubMed](#)]
86. Yamaguchi, A.; Nakashima, R.; Sakurai, K. Structural basis of RND-type multidrug exporters. *Front. Microbiol.* **2015**, *6*, 327. [[CrossRef](#)] [[PubMed](#)]
87. Chevalier, J.; Atifi, S.; Eyraud, A.; Mahamoud, A.; Barbe, J.; Pagès, J.M. New pyridoquinoline derivatives as potential inhibitors of the fluoroquinolone efflux pump in resistant *Enterobacter aerogenes* strains. *J. Med. Chem.* **2001**, *44*, 4023–4026. [[CrossRef](#)]
88. Alekshun, M.N.; Levy, S.B. Regulation of chromosomally mediated multiple antibiotic resistance: The mar regulon. *Antimicrob. Agents Chemother.* **1997**, *41*, 2067–2075. [[CrossRef](#)]
89. Keeney, D.; Ruzin, A.; McAleese, F.; Murphy, E.; Bradford, P.A. MarA-mediated overexpression of the AcrAB efflux pump results in decreased susceptibility to tigecycline in *Escherichia coli*. *J. Antimicrob. Chemother.* **2008**, *61*, 46–53. [[CrossRef](#)]
90. Gallo, S.; Chevalier, J.; Mahamoud, A.; Eyraud, A.; Pagès, J.M.; Barbe, J. 4-alkoxy and 4-thioalkoxyquinoline derivatives as chemosensitizers for the chloramphenicol-resistant clinical *Enterobacter aerogenes* 27 strain. *Int. J. Antimicrob. Agents* **2003**, *22*, 270–273. [[CrossRef](#)]
91. Malléa, M.; Mahamoud, A.; Chevalier, J.; Alibert-Franco, S.; Brouant, P.; Barbe, J.; Pages, J.-M. Alkylaminoquinolines inhibit the bacterial antibiotic efflux pump in multidrug-resistant clinical isolates. *Biochem. J.* **2003**, *376*, 801–805. [[CrossRef](#)]
92. Lamers, R.P.; Cavallari, J.F.; Burrows, L.L. The Efflux Inhibitor Phenylalanine-Arginine Beta-Naphthylamide (PAβN) Permeabilizes the Outer Membrane of Gram-Negative Bacteria. *PLoS ONE* **2013**, *8*, e60666. [[CrossRef](#)]
93. Chevalier, J.; Bredin, J.; Mahamoud, A.; Malléa, M.; Barbe, J.; Pagès, J.M. Inhibitors of Antibiotic Efflux in Resistant *Enterobacter aerogenes* and *Klebsiella pneumoniae* Strains. *Antimicrob. Agents Chemother.* **2004**, *48*, 1043–1046. [[CrossRef](#)]
94. Ghisalberti, D.; Mahamoud, A.; Chevalier, J.; Baitiche, M.; Martino, M.; Pagès, J.M.; Barbe, J. Chloroquinolines block antibiotic efflux pumps in antibiotic-resistant *Enterobacter aerogenes* isolates. *Int. J. Antimicrob. Agents* **2006**, *27*, 565–569. [[CrossRef](#)]
95. Machado, D.; Fernandes, L.; Costa, S.S.; Cannalire, R.; Manfroni, G.; Tabarrini, O.; Couto, I.; Sabatini, S.; Viveiros, M. Mode of action of the 2-phenylquinoline efflux inhibitor PQQ4R against *Escherichia coli*. *PeerJ* **2017**, *5*, e3168. [[CrossRef](#)] [[PubMed](#)]
96. Cadelis, M.M.; Li, S.A.; Bourguet-Kondracki, M.-L.; Blanchet, M.; Douafer, H.; Brunel, J.M.; Copp, B.R. Spermine Derivatives of Indole-3-carboxylic Acid, Indole-3-acetic Acid and Indole-3-acrylic Acid as Gram-Negative Antibiotic Adjuvants. *ChemMedChem* **2021**, *16*, 513–523. [[CrossRef](#)] [[PubMed](#)]
97. Zhang, Z.; Pang, Y.; Wang, Y.; Cohen, C.; Zhao, Y.; Liu, C. Differences in risk factors and drug susceptibility between *Mycobacterium avium* and *Mycobacterium intracellulare* lung diseases in China. *Int. J. Antimicrob. Agents* **2015**, *45*, 491–495. [[CrossRef](#)]
98. Jones, M.M.; Winthrop, K.L.; Nelson, S.D.; Duvall, S.L.; Patterson, O.V.; Nechodom, K.E.; Findley, K.E.; Radonovich, L.J., Jr.; Samore, M.H.; Fennelly, K.P. Epidemiology of nontuberculous mycobacterial infections in the U.S. Veterans Health Administration. *PLoS ONE* **2018**, *13*, e0197976. [[CrossRef](#)] [[PubMed](#)]
99. Schmalstieg, A.M.; Srivastava, S.; Belkaya, S.; Deshpande, D.; Meek, C.; Leff, R.; Van Oers, N.S.C.; Gumbo, T. The antibiotic resistance arrow of time: Efflux pump induction is a general first step in the evolution of mycobacterial drug resistance. *Antimicrob. Agents Chemother.* **2012**, *56*, 4806–4815. [[CrossRef](#)] [[PubMed](#)]
100. Rodrigues, L.; Sampaio, D.; Couto, I.; Machado, D.; Kern, W.V.; Amaral, L.; Viveiros, M. The role of efflux pumps in macrolide resistance in *Mycobacterium avium* complex. *Int. J. Antimicrob. Agents* **2009**, *34*, 529–533. [[CrossRef](#)]

101. Rodrigues, L.; Ramos, J.; Couto, I.; Amaral, L.; Viveiros, M. Ethidium bromide transport across *Mycobacterium smegmatis* cell-wall: Correlation with antibiotic resistance. *BMC Microbiol.* **2011**, *11*, 35. [[CrossRef](#)]
102. Rodrigues, L.; Wagner, D.; Viveiros, M.; Sampaio, D.; Couto, I.; Vavra, M.; Kern, W.V.; Amaral, L. Thioridazine and chlorpromazine inhibition of ethidium bromide efflux in *Mycobacterium avium* and *Mycobacterium smegmatis*. *J. Antimicrob. Chemother.* **2008**, *61*, 1076–1082. [[CrossRef](#)]
103. Lechner, D.; Gibbons, S.; Bucar, F. Plant phenolic compounds as ethidium bromide efflux inhibitors in *Mycobacterium smegmatis*. *J. Antimicrob. Chemother.* **2008**, *62*, 345–348. [[CrossRef](#)] [[PubMed](#)]
104. Rindi, L. Efflux Pump Inhibitors against Nontuberculous Mycobacteria. *Int. J. Mol. Sci.* **2020**, *21*, 4191. [[CrossRef](#)] [[PubMed](#)]
105. Cannalire, R.; Machado, D.; Felicetti, T.; Santos Costa, S.; Massari, S.; Manfroni, G.; Barreca, M.L.; Tabarrini, O.; Couto, I.; Viveiros, M.; et al. Natural isoflavone biochanin A as a template for the design of new and potent 3-phenylquinolone efflux inhibitors against *Mycobacterium avium*. *Eur. J. Med. Chem.* **2017**, *140*, 321–330. [[CrossRef](#)] [[PubMed](#)]
106. Felicetti, T.; Machado, D.; Cannalire, R.; Astolfi, A.; Massari, S.; Tabarrini, O.; Manfroni, G.; Barreca, M.L.; Cecchetti, V.; Viveiros, M.; et al. Modifications on C6 and C7 Positions of 3-Phenylquinolone Efflux Pump Inhibitors Led to Potent and Safe Antimycobacterial Treatment Adjuvants. *ACS Infect. Dis.* **2019**, *5*, 982–1000. [[CrossRef](#)]
107. Yoshida, K.-I.; Nakayama, K.; Ohtsuka, M.; Kuru, N.; Yokomizo, Y.; Sakamoto, A.; Takemura, M.; Hoshino, K.; Kanda, H.; Nitana, H.; et al. MexAB-OprM specific efflux pump inhibitors in *Pseudomonas aeruginosa*. Part 7: Highly soluble and in vivo active quaternary ammonium analogue D13-9001, a potential preclinical candidate. *Bioorg. Med. Chem.* **2007**, *15*, 7087–7097. [[CrossRef](#)] [[PubMed](#)]
108. Wang, Z.; Fan, G.; Hryc, C.F.; Blaza, J.N.; Serysheva, I.I.; Schmid, M.F.; Chiu, W.; Luisi, B.F.; Du, D. An allosteric transport mechanism for the AcrAB–TolC multidrug efflux pump. *Elife* **2017**, *6*, e24905. [[CrossRef](#)]
109. Glavier, M.; Puvanendran, D.; Salvador, D.; Decossas, M.; Phan, G.; Garnier, C.; Frezza, E.; Cece, Q.; Schoehn, G.; Picard, M.; et al. Antibiotic export by MexB multidrug efflux transporter is allosterically controlled by a MexA-OprM chaperone-like complex. *Nat. Commun.* **2020**, *11*, 4948. [[CrossRef](#)]